Single-vortex fluctuations in layered superconductors: Electromagnetic coupling and crossover to strong pinning

Jan Kierfeld
Max-Planck-Institut für Kolloid- und Grenzflächenforschung, 14424 Potsdam, Germany
(Received 14 March 2003; revised manuscript received 29 January 2004; published 16 April 2004)

Positional fluctuations of single vortices induced by thermal fluctuations and random point pinning are considered in detail for all length scales fully taking into account the competing effects of Josephson and electromagnetic coupling between vortex elements. The electromagnetic coupling gives rise to a pronounced dispersion of the line stiffness and soft short-wavelength modes which modify the displacement fluctuations of the pinned vortex over a wide range of length scales. Furthermore, we present a detailed analysis of strongly pinned individual pancake vortices in a layered superconductor and study the crossover to the collectively pinned single-vortex line. The line stiffness dispersion leads to sharp increases in the pinning length at characteristic temperatures both for weak and strong pinning and two crossover scales. We calculate as well the corresponding increase in the characteristic pinning energy and the pronounced drop of the critical current at these characteristic temperatures. We predict distinct features in the current-voltage characteristics due to the effects of strong pinning and vortex line tension dispersion.

DOI: 10.1103/PhysRevB.69.144513 PACS number(s): 74.25.Qt, 74.25.Sv

I. INTRODUCTION

The physics of single vortices pinned by point defects in a type-II superconductor is one of the best studied problems in the context of vortex physics as well as the statistical physics of disordered systems.[1–3] Nevertheless, there are still some important aspects, which have been neglected in earlier theoretical studies but deserve further consideration. One of these aspects is the influence of the nonlocal electromagnetic interaction along the vortex line on the statistical physics on larger scales, in particular, regarding the positional fluctuations of the vortex line induced by quenched point disorder and its dynamic behavior in the presence of external currents. In a layered type-II superconductor, another aspect is the crossover from collectively pinned long vortex line segments containing many pancake segments for small point defect concentrations to strongly pinned single-pancake segments at high point defect concentrations.

The electromagnetic coupling of segments along a vortex line leads to strongly nonlocal elastic properties of a vortex line below the magnetic penetration depth λ_{ab}, which sets the range of the electromagnetic coupling. Furthermore, the interplay between electromagnetic coupling and Josephson coupling sets a preferred length scale $\varepsilon\lambda_{ab}$ for short-wavelength fluctuations of the vortex line, where $\varepsilon = \lambda_{ab}/\lambda_c$ is the anisotropy ratio of the type-II superconductor. For high-temperature superconductors (HTSC) such as $YBa_2Cu_3O_{7-\delta}$ (YBCO) or $Bi_2Sr_2CaCu_2O_{8+\delta}$ (BSCCO) this leads to particularly interesting crossover phenomena because the layered structure with layer distance d sets a competing shortest length scale for vortex line fluctuations. These two length scales govern much of the statistical physics of purely thermal fluctuations of single vortex lines.

Pinning by point defects introduces yet another relevant length scale, the collective pinning length L_c of a weakly pinned vortex line. Moreover, thermal fluctuations lead to an effective weakening of the pinning strength which can give rise to a thermal depinning and a pronounced temperature dependence of the pinning length. Much of the present paper is devoted to the detailed study of the various crossover phenomena that arise due to the presence of up to four relevant length scales λ_{ab}, $\varepsilon\lambda_{ab}$, d, and L_c which can become comparable in size for HTSC materials depending on anisotropy and pinning strength. Depending on the size of L_c as compared to the length scales $\varepsilon\lambda_{ab}$ and d there is a crossover from collectively pinned long vortex line segments for weak pinning potentials (small point defect concentration) to strongly pinned short segments at higher disorder strengths (high point defect concentration). Therefore, the electromagnetic coupling also has a strong effect on the pinning of single vortices. If in a layered HTSC L_c becomes smaller than the layer spacing d we enter a qualitatively different regime of strong pinning, where the perturbative treatment of pinning forces breaks down even for single-pancake segments.

Whereas there is extensive literature on the weak collective pinning theory since the pioneering work of Larkin and Ovchinnikov,[4] the crossover to strong pinning of single pancakes and the implications of the electromagnetic coupling for pinning are much less studied although they are technologically relevant for HTSC.[5] For the layered HTSC materials we will discuss in detail the crossover from fluctuations of linelike one-dimensional vortex segments to fluctuations of pointlike pancake vortices upon increasing the pinning strength. For BSCCO there have been a number of experimental studies[6–8] of this crossover behavior. Theoretical investigations[9] have focused as well on the BSCCO compound and treated the limit of a vanishing Josephson coupling of superconducting layers, i.e., $\varepsilon = 0$. In this decoupled limit pancake vortices in different layers interact only electromagnetically. In Ref. 9 it has been shown that in the decoupled limit the crossover between pointlike and linelike pinning leads to a sharp drop of the critical current if temperature is increased which can also give rise to a two-step

behavior in the current-voltage characteristics at fixed temperature.

In this paper, we present a more detailed theoretical analysis of the effects of the nonlocal electromagnetic coupling on the pinning of single vortices and of strongly pinned single vortices which also extends to the more realistic situation of a *finite* Josephson coupling between the layers. This allows one to apply our results to the strongly layered BSCCO compound where $\varepsilon\lambda_{ab} \ll d$ as well as to the YBCO compound where the Josephson coupling is much larger such that $\varepsilon\lambda_{ab}$ becomes comparable to the layer spacing d. Qualitative differences between these materials are worked out by our analysis. Our results are also valid in the limit of small layer spacing $d \ll \varepsilon\lambda_{ab}$. Then the layer spacing drops out as a relevant length scale, and we cross over to a description of anisotropic type-II superconductors.

We give a complete account of crossover phenomena related to the interplay between Josephson coupling and electromagnetic coupling in the vortex line tension on the one hand, and the interplay of pinning by point defects and thermal motion of the vortex elements on the other hand. We study these crossover phenomena in the positional fluctuations of the vortex line, the pinning length, the associated critical currents, and the current-voltage characteristics. We present a detailed and complete calculation of the mean-square vortex displacements due to quenched point disorder and thermal fluctuations for single-vortex segments of arbitrary length L. The electromagnetic coupling gives rise to a pronounced dispersion of the line stiffness which leads to the appearance of soft short-wavelength modes on scales which modify the displacement fluctuations of the pinned vortex over a wide range of length scales. Thermal as well as disorder-induced positional fluctuations exhibit a rich crossover behavior as the vortex length L passes through the four relevant length scales $\varepsilon\lambda_{ab}$, d, λ_{ab}, and L_c. Furthermore the dispersion leads to a breakdown of self-affine scaling of vortex displacements and the emergence of two additional crossover scales.

Using our results for the positional fluctuations of vortex segments we demonstrate that sharp increases in the pinning length and drops in the critical current upon increasing the temperature should be observable also in the presence of a finite Josephson coupling as for YBCO, and even in anisotropic type-II superconductors in the low-field regime. We also predict distinct jumplike features in the current-voltage characteristics in these materials at sufficiently high impurity concentration. Moreover, positional fluctuations of single vortices are of great interest for estimates based on the Lindemann criterion regarding the stability of a topologically ordered vortex *lattice* with respect to thermal fluctuations[10] or random point pinning.[11] In particular, results presented in this paper will be of further use in obtaining a correct picture of the low-field part of the vortex phase diagram of layered type-II superconductors.

The paper is organized as follows. In Sec. II we introduce the nonlocal elasticity of single vortices due to the electromagnetic coupling. These results can be employed to discuss purely thermal fluctuations in Sec. III and fluctuations due to quenched point disorder at $T=0$ in Sec. IV. Weak collective pinning of vortex lines at $T=0$ is discussed in Sec. IV A and the crossover to strong pinning of individual pancake vortices in Sec. IV B before we consider the pinning of long vortex segments in Sec. IV C. For finite temperatures thermal fluctuations start to smear out the pinning energy landscape giving finally rise to thermal depinning of the vortex line, which is discussed in Sec. V. Also in this section, we first discuss the thermal depinning of a weakly pinned vortex line in Sec. V A, afterwards the thermal depinning from strong pinning in Sec. V B, and finally the thermal depinning of long vortex segments in Sec. V C. These results can be applied to calculate energy barriers for the motion of single vortices in the presence of an external current j. This allows one to calculate single-vortex critical currents in Sec. VI and discuss features of the current-voltage characteristics in Sec. VII. A list of symbols is provided in Table I.

II. ELECTROMAGNETIC COUPLING AND NONLOCAL STIFFNESS

A single vortex can be described as a line under tension with a stiffness ε_l. The exact form of the line stiffness depends not only on material parameters such as the magnetic penetration depth λ_{ab}, the anisotropy ratio $\varepsilon=\lambda_{ab}/\lambda_c$, or the Ginzburg-Landau parameter $\kappa=\lambda_{ab}/\xi_{ab}$ but also on the wavelength of the fluctuations that are considered. This is because the electromagnetic interaction is nonlocal and extends over a range λ_{ab} for the usual geometry $\mathbf{H}\|\mathbf{c}$ also considered in this paper. Therefore, the elastic tilt energy of the vortex line becomes nonlocal. In the presence of an external pinning potential the Hamiltonian of the single vortex line of length L is

$$\mathcal{H}=\int_0^L dz \int_0^L dz' \left\{ \frac{1}{2}\varepsilon_l(z-z')\partial_z \mathbf{u}(z)\cdot\partial_z \mathbf{u}(z') + \delta(z-z')V(z,\mathbf{u}(z)) \right\}. \tag{1}$$

The vortex line configurations are parametrized by a two-component displacement field $\mathbf{u}(z)$ (when commenting on the general case we will denote the number of components by n), where z is the coordinate along the equilibrium direction of the vortex line which is parallel to $\mathbf{H}\|\mathbf{c}$. Pinning potentials V are specified later on. $\varepsilon_l(z)$ is the nonlocal vortex stiffness, and after Fourier transforming $\varepsilon_l(q)=\int dz \varepsilon_l(z) e^{iqz}$ we obtain the dispersion relation of the line stiffness. In the limit of an isolated vortex line the dispersive line tension is[2]

$$\varepsilon_l(q) \approx \frac{\varepsilon_0}{2}\left[\varepsilon^2 \ln\left(\frac{1}{\xi_c^2 q^2}\right) + \frac{1}{q^2\lambda_{ab}^2}\ln\left(1+\frac{q^2\lambda_{ab}^2}{1+q^2u^2}\right)\right], \tag{2}$$

where $\varepsilon_0=(\Phi_0/4\pi\lambda_{ab})^2$ is the characteristic line energy of a vortex. The first term stems from the Josephson coupling

TABLE I. List of symbols. Our notation is mostly adapted from Ref. 1.

a	Vortex lattice spacing	
γ	Pinning strength parameter	Eq. (13)
d	Layer spacing	
E_0	Pancake ground-state energy	Eq. (29)
δ	Pinning strength parameter	Eq. (14)
δ_d	Layered pinning strength parameter	Eq. (16)
$\varepsilon=\lambda_{ab}/\lambda_c$	Anisotropy ratio	
ε_d	Layered anisotropy	Eq. (5)
$\varepsilon_l(q)$	(Dispersive) single-vortex line tension	Eqs. (2) and (3)
$\varepsilon_0=(\Phi_0/4\pi\lambda_{ab})^2$	Line energy	
j_c	Critical current	Eqs. (77)–(80), (83), and (86)
j_d	Strong pinning current strength	Eq. (81)
j^*	Pancake barrier current	Eqs. (82) and (86)
$\tilde{L}$	Thermal plateau length	Eq. (11)
$\tilde{L}_c$	Pinning plateau length	Eqs. (21) and (36)
L_c	Collective pinning or Larkin length	Eqs. (22), (23), (46), and (51)
L_d	Dispersion length scale	Eq. (4)
L_0	Single-vortex length	Eq. (8)
$T_{dp,\varepsilon}$	Anisotropic depinning temperature	Eq. (47)
$T_{dp,\varepsilon\lambda}$	Depinning temperature for the scales $\varepsilon\lambda_{ab}$, $\tilde{L}$	Eq. (49)
$T_{dp,i}$	Isotropic depinning temperature	Eqs. (50) and (54)
$T_{dp,d}$	Depinning temperature for weakly pinned pancake vortices	Eq. (52)
$T_{\varepsilon\lambda}$	Temperature where $L_c(T)=\varepsilon\lambda_{ab}$	Eq. (48)
T_d	Temperature where $L_c(T)=d$ from weak collective pinning	Eq. (53)
$T_{d,J}$	Crossover temperature to strong Josephson coupling	Eq. (6)
$T^*=U^*$	Pancake thermal activation temperature	Eq. (61)
U_c	Pinning energy variation	Eqs. (75), (84), and (85)
U_p	Pancake pinning energy	Eq. (15)
U^*	Pancake energy barrier	Eq. (30)

between the line elements and is local whereas the second term originates from the electromagnetic interaction of line elements, and is strongly nonlocal. u is a typical displacement, and the corresponding correction term in the expression (2) is due to nonlinear elastic effects. In the local limit (for wave vectors $q<1/\lambda_{ab}$), the electromagnetic part dominates, and the stiffness is nondispersive $\varepsilon_l\simeq\varepsilon_0$ ($\simeq$ is used if numerical prefactors or small logarithmic corrections are neglected). On the smallest scales ($q>1/\varepsilon\lambda_{ab}$), the Josephson contribution dominates and we find an essentially nondispersive but anisotropic stiffness $\varepsilon_l\simeq\varepsilon_0\varepsilon^2$, which is reduced by a factor ε^2 as compared to the electromagnetic large-scale result [we neglect the small logarithmic correction due to the weakly dispersive factor $\ln(1/\xi_c^2q^2)$ in the following]. On intermediate scales $1/\lambda_{ab}<q<1/\varepsilon\lambda_{ab}$ the electromagnetic coupling dominates but it is reduced by dispersion until it is finally cut off by the Josephson contribution at $q\approx1/\varepsilon\lambda_{ab}$. In this regime we find $\varepsilon_l\simeq\varepsilon_0/q^2\lambda_{ab}^2$. In the following we will therefore use these simplified expression

$$\varepsilon_l(q)\simeq\begin{cases} q<\dfrac{1}{\lambda_{ab}}: & \varepsilon_0 \\ \dfrac{1}{\lambda_{ab}}<q<\dfrac{1}{\varepsilon\lambda_{ab}}: & \dfrac{\varepsilon_0}{q^2\lambda_{ab}^2} \\ q>\dfrac{1}{\varepsilon\lambda_{ab}}: & \varepsilon_0\varepsilon^2, \end{cases} \tag{3}$$

which is justified if prefactors and logarithmic corrections can be neglected. In the limit of a very weak Josephson coupling $\varepsilon\to0$ the dispersion of the electromagnetic contribution persists down to the shortest length scale, which is set by the layer distance d. For the fluctuation behavior the largest possible wave vector showing q^{-2} dispersion is important. In a layered material this is $q_d\simeq1/\max\{d,\varepsilon\lambda_{ab}\}$ and we introduce a corresponding *dispersion length scale*

$$L_d=\max\{d,\varepsilon\lambda_{ab}\}=\lambda_{ab}\max\{\varepsilon_d,\varepsilon\}, \tag{4}$$

where

$$\varepsilon_d = \frac{d}{\lambda_{ab}} \tag{5}$$

is an effective *layered anisotropy* of the material. For the short-scale fluctuations it is important to distinguish between two classes of type-II superconductors depending on the strength of the Josephson coupling or the size of ε. Layered superconductors with a *strong* Josephson coupling $\varepsilon > \varepsilon_d$ have $L_d \simeq \varepsilon \lambda_{ab}$. One prominent example of this class is YBCO. *Formally*, we can also treat anisotropic type-II superconductors which have no layered structure (and thus there is no Josephson coupling) within this class of materials if we set $d=0$. On the other hand, superconductors with a *weak* Josephson coupling $\varepsilon < \varepsilon_d$ have $L_d \simeq d$. But it has to be noted that even if $\varepsilon < \varepsilon_d$ at $T=0$ the Josephson coupling becomes strong above a reduced temperature

$$t_{d,J} = 1 - (\varepsilon/\varepsilon_d)^2 \tag{6}$$

because $\varepsilon_d \propto (1-t)^{1/2}$. For typical parameters for BSCCO, $\varepsilon \approx 1/200$, $d \approx 15$ Å, $\lambda_{ab} \approx 2000$ Å, and $T_c \approx 100$ K one finds that BSCCO has a weak Josephson coupling at low temperatures but the Josephson coupling becomes strong above $T_{d,J} \approx 55$ K. An estimate for the stiffness on the short scale L_d is $\varepsilon_l(q_d) \simeq \varepsilon_0 L_d^2/\lambda_{ab}^2 \simeq \varepsilon_0 \max\{\varepsilon_d^2, \varepsilon^2\}$ from Eq. (3) or somewhat more accurate $\varepsilon_l(q_d) \simeq \varepsilon_0(\varepsilon^2 + \max\{\varepsilon_d^2, \varepsilon^2\})$ from Eq. (2).

Considering only fluctuations with wave vectors $1/\lambda_{ab} < q < q_d$ in the Fourier transform the elastic part of the Hamiltonian (1) can be written as

$$\mathcal{H} \simeq \int_0^{\lambda_{ab}} \frac{dz}{L_d} \left\{ \frac{1}{2} \frac{\varepsilon_0}{\lambda_{ab}^2} u(z)^2 \right\}, \tag{7}$$

i.e., due to the predominantly electromagnetic coupling each vortex segment of length λ_{ab} effectively *decouples* into small segments of length L_d that fluctuate independently in a harmonic potential.[12] Therefore, the vortex line becomes very soft with respect to fluctuations on the short scale L_d. This holds for thermal fluctuations as well as for fluctuations due to pinning by point defects.

In this paper we consider the pinning of *isolated* vortices of length L. Also in a vortex *lattice* vortices fluctuate essentially as isolated vortex lines if L is sufficiently small that they are not yet limited in their fluctuations by the interaction with the neighboring lines. This happens as the shear energy $c_{66} u^2 L$ becomes comparable to the tilt energy $\varepsilon_l (1/L) u^2/L$. For a vortex lattice constant a, the shear modulus is given by $c_{66} \simeq \varepsilon_0/a^2$ in the dense regime $a < \lambda_{ab}$ and $c_{66} \simeq (\varepsilon_0/a^2)(a/\lambda_{ab})^{3/2} \exp(-a/\lambda_{ab})$ in the dilute limit $a > \lambda_{ab}$. Therefore, we find single-vortex behavior also in a vortex lattice on scales smaller than the *single-vortex length*

$$L_0 \simeq a \left(\frac{\varepsilon_l(1/L_0)}{c_{66}} \right)^{1/2} \simeq \begin{cases} a < \lambda_{ab}: & \varepsilon a \\ a > \lambda_{ab}: & a(\lambda_{ab}/a)^{3/4} \exp(a/2\lambda_{ab}). \end{cases} \tag{8}$$

Note that even in the dense limit where vortices already have a considerable magnetic interaction we still find single-vortex physics on sufficiently small scales $L < L_0$ which defines the range of applicability of our results. Thus the effects of the dispersion in the line stiffness (3) of a single vortex will become relevant if $L_d < L_0$. For a layered HTSC with strong Josephson coupling such as YBCO or for anisotropic type-II superconductors where $L_d = \varepsilon \lambda_{ab}$ dispersion effects are thus relevant in the low-field regime $a > \lambda_{ab}$ or $B < \Phi_0/\lambda_{ab}^2$. For YBCO with $\lambda_{ab} \approx 1500$ Å this low-field range is $B < 900$ G. For strongly layered HTSC's with a weak Josephson coupling such as BSCCO we have $L_d = d$ (for $t < t_d$) and effects from the dispersion become important in the regime $L_0 > d$, which is again approximately the low-field regime $B < \Phi_0/\lambda_{ab}^2$ due to the exponential increase of L_0 in this regime.[14] For BSCCO with $\lambda_{ab} \approx 2000$ Å this low-field regime is $B < 500$ G. Within these low-field ranges the effects from the electromagnetic coupling within a single vortex, which we will present in the remainder of the paper, should be experimentally observable.

III. THERMAL FLUCTUATIONS

It is instructive to consider first how the electromagnetic softening affects thermal fluctuations [i.e., $V=0$ in Eq. (1)] of a vortex line of length L. Using the expression (3) for the stiffness one finds up to irrelevant corrections

$$\langle u^2 \rangle_T(L) \simeq 2 \int_{1/L}^{1/d} \frac{dq}{2\pi} \frac{T}{\varepsilon_l(q) q^2} \simeq \begin{cases} d < L < \varepsilon \lambda_{ab}: & \dfrac{TL}{\varepsilon_0 \varepsilon^2} \\ L_d < L < \lambda_{ab}: & \langle u^2 \rangle_T(L_d) \simeq \dfrac{TL_d}{\varepsilon_l(q_d)} \\ L > \lambda_{ab}: & \dfrac{TL}{\varepsilon_0} + \dfrac{TL_d}{\varepsilon_l(q_d)}, \end{cases} \tag{9}$$

where $\langle \cdots \rangle_T$ is the purely thermal average setting $V=0$. [The relative displacement $\langle [u(L)-u(0)]^2 \rangle_T$ along an infinite line is larger than the mean-square displacement $\langle u^2 \rangle_T(L)$ of a finite segment of length L with fixed center of mass by a numerical prefactor, but the parameter dependence is identical]. Apart from numerical prefactors the formula (9) holds for general n-component fields $\mathbf{u}(z)$. If the electromagnetic stiffness contribution dominates, the thermal displacements $\langle u^2 \rangle_T(L)$ are approximately *independent* of L for $L_d < L < \lambda_{ab}$ due to the effective decoupling. The result is a *plateau* in the thermal displacements $\langle u^2 \rangle_T(L)$ over a certain range of scales L. On scales $L > L_d$, the thermally fluctuating vortex line is therefore no longer self-affine with a roughness exponent $\zeta_T = 1/2$ but, instead, we have to explicitly include soft short-scale fluctuations on the scale L_d as we did in the last line of Eq. (9). It is easy to check that all dispersion relations $\varepsilon_l(q) \propto q^{-\omega}$ with $\omega > 1$ would formally lead to a

negative $\zeta_T=(1-\omega)/2<0$ such that self-affinity is lost. As a consequence we can write the last line of Eq. (9) for $L>\lambda_{ab}$ as

$$\langle u^2\rangle_T(L)\simeq\langle u^2\rangle_{T,q<\lambda}(L)+\langle u^2\rangle_T(L_d)\simeq\langle u^2\rangle_T(L_d)\left(\frac{L}{\tilde{L}}+1\right), \tag{10}$$

where the subscript "$q<\lambda$" implies that only small wave vectors $q<\lambda_{ab}$ are integrated over and thus the average is performed using the isotropic stiffness $\varepsilon_l(q)\simeq\varepsilon_0$ according to Eq. (2). From formula (10) we read off that short-scale fluctuations actually dominate for all scales $L_d<L<\tilde{L}$ with

$$\tilde{L}\simeq L_d\frac{\varepsilon_0}{\varepsilon_l(q_d)}\simeq\frac{\lambda_{ab}^2}{L_d}\simeq\frac{\lambda_{ab}}{\max\{\varepsilon_d,\varepsilon\}}. \tag{11}$$

Therefore, $L_d<L<\tilde{L}$ gives the extent of the plateau in the thermal displacements and the *thermal plateau length* $\tilde{L}$ is the crossover length scale where self-affinity breaks down and both contributions in Eq. (10) are equal. We will encounter a similar breakdown of self-affinity also in the case of fluctuations induced by point disorder.

Let us briefly comment on implications for the thermal melting of the vortex lattice in order to demonstrate the importance of the plateau length scale $\tilde{L}$ also for vortex lattice properties. Using the single-vortex length L_0, we can reformulate the Lindemann criterion for thermal melting in a single-vortex form[13,14]

$$\langle u^2\rangle_T(L_0)=c_L^2a^2, \tag{12}$$

with the Lindemann number $c_L\approx 0.1-0.2$. In the dilute limit $L_0\gg\lambda_{ab}$ and we actually have to use the last line of Eq. (9) to calculate the left-hand side of Eq. (12). Due to the soft electromagnetic coupling both contributions from $L\simeq L_0$ and $L\simeq L_d$ can melt the lattice which leads to the existence of *two* branches of the melting line in the dilute regime, the upper branch due to fluctuations on the short scale $L\simeq L_d$ and the lower branch due to fluctuations on the large scale $L\simeq L_0$. A detailed analysis of the resulting melting curves[14] reproduces the results of Ref. 15. Moreover, the thermal plateau scale $\tilde{L}$ is intimately related to the location of the "tip" of the melting curve: If L_0 equals the thermal plateau length $\tilde{L}$, i.e., $L_0\simeq\tilde{L}$ both contributions are equal and thus this condition determines the location of the tip of the melting curve. This makes clear that much of the phase behavior of the vortex lattice is already encoded in the single-vortex properties and that it is the nonlocal electromagnetic coupling along a single vortex line which gives rise to the complex phase behavior in the low-field regime. Calculations regarding the resulting phase diagrams for vortex lattices are presented elsewhere,[14] in this work we focus on single-vortex properties.

IV. VORTEX PINNING AT $T=0$

Now, we consider fluctuations of a single vortex line caused by quenched point defects at low temperatures $T\approx 0$ such that we can neglect thermal fluctuations. The effect of point defects can be modeled by a quenched disorder potential $V(z,\mathbf{u})$ with a Gaussian distribution, zero mean, and short-range correlations in all directions,[3]

$$\begin{aligned}\overline{V(z,\mathbf{u})V(z',\mathbf{u}')}&=\gamma\xi_{ab}^4\delta(z-z')\delta_{\xi_{ab}}(\mathbf{u}-\mathbf{u}')\\&=\gamma\xi_{ab}^4\delta(z-z')\int\frac{d^2K}{(2\pi)^2}e^{-K^2\xi_{ab}^2}\\&\quad\times e^{i\mathbf{K}\cdot(\mathbf{u}-\mathbf{u}')}.\end{aligned} \tag{13}$$

The parameter γ gives the strength of the quenched disorder and is temperature dependent.[1] As indicated in Eq. (13) the δ function is smeared out to a range ξ_{ab} given by the size of the vortex cores, which can be modeled using the Fourier representation of a Gaussian in the second line. A convenient *pinning strength parameter* δ (see Ref. 1) is defined by the ratio of the mean-square pinning energy for a small line element of length $L\simeq\xi_c$ and with typical displacement $u\simeq\xi_{ab}$, $E_{\rm pin}^2(\xi_c)\simeq\gamma\xi_{ab}^2\xi_c$, and the square of the corresponding tilt energy $E_{\rm tilt}(\xi_c)\simeq\varepsilon_0\varepsilon^2\xi_{ab}^2/\xi_c\simeq\varepsilon_0\xi_c$,

$$\frac{\delta}{\varepsilon}=\frac{\gamma\xi_{ab}^2\xi_c}{(\varepsilon_0\xi_c)^2}. \tag{14}$$

In a layered material one can consider the analogous energies for a segment of length $L\simeq d$, i.e., the mean-square pinning energy $E_{\rm pin}^2(d)\simeq U_p^2$ with the *pancake pinning energy*

$$U_p=(\gamma\xi_{ab}^2d)^{1/2} \tag{15}$$

and the square of the corresponding tilt energy $E_{\rm tilt}(d)\simeq\varepsilon_l(1/d)\xi_{ab}^2/d\simeq\varepsilon_0(\varepsilon^2+\varepsilon_d^2)\xi_{ab}^2/d$, see Eq. (2). Using this we define an analogous *layered pinning strength parameter* δ_d as

$$\delta_d=\frac{U_p^2}{[\varepsilon_0(\varepsilon^2+\varepsilon_d^2)\xi_{ab}^2/d]^2}. \tag{16}$$

From the definitions it is clear that collective pinning theory applies to weak pinning $\delta/\varepsilon\ll 1$ and $\delta_d\ll 1$. Whereas the former condition is usually fulfilled in anisotropic HTSC's such as YBCO the latter is violated in layered HTSC's with strong disorder such as BSCCO. We call pinning with $\delta_d>1$ *strong pinning*, which we will discuss in detail in Sec. IV B.

A. Weak collective pinning

First we want to focus on the pinning of vortex *lines* at low temperatures. This required to consider segments of length $L>d$. Segments with a length comparable to d have to be treated as pointlike pancake vortices, the disorder-induced fluctuations of which will be discussed in Sec. IV B. The physics of a single vortex line in point disorder exhibits two different scaling regimes depending on the typical size of the disorder-induced mean-square displacement $\overline{\langle u\rangle^2}(L)$ of a vortex segment of length L. For short vortex lengths

displacements are small $\overline{\langle u\rangle^2}(L)<\xi_{ab}^2$, perturbation theory is valid, and we can work with Larkin's random forces.[4] Fluctuations around the ground state of the line are *Gaussian* in this *random force* (RF) regime and we find a roughness exponent $\zeta_{RF}=3/2$, i.e., $\overline{\langle u\rangle^2}(L)\propto L^3$ for all n. This regime is valid up to the *collective pinning* or *Larkin length* L_c which is defined by the condition $\overline{\langle u\rangle^2}(L_c)=\xi_{ab}^2$. Longer segments explore many almost degenerate minima of the pinning energy landscape such that fluctuations are non-Gaussian. In this so-called *random manifold* (RM) regime the roughness exponent is known exactly only for $n=1$ where $\zeta_{RM}=2/3$.[16] The currently most reliable estimate for general n is $\zeta_{RM}=(3+n)/2(2+n)$ (Ref. 17 and 18) giving $\zeta_{RM}=5/8$ for the vortex line in the bulk superconductor. Therefore we find $\overline{\langle u\rangle^2}(L)\propto L^{5/4}$ as the asymptotic limit for large L. However, these results were derived for a dispersion-free stiffness and apply in this form only to length scales $L<\varepsilon\lambda_{ab}$ where we can neglect the dispersive electromagnetic coupling or on very large scales $L\gg\lambda_{ab}$ where the local limit of the electromagnetic coupling dominates. In this section we want to explore the consequences of the electromagnetic coupling on the scaling properties of $u(L)$ for line pinning with $L>d$. In particular, we consider only $L_c>d$, as $L_c=d$ marks the boundary to the regime of pancake vortex pinning. From the definition of δ_d [see Eq. (16)] and L_c it becomes clear that $L_c=d$ is equivalent to $\delta_d=1$ and thus also marks the onset of strong pinning.

On small scales $L<L_c$, where $\overline{\langle u\rangle^2}(L)<\xi_{ab}^2$, we expand $V(z,\mathbf{u})$ about $\mathbf{u}=0$ to find Gaussian distributed random forces $\mathbf{f}(z)$ with

$$V(z,\mathbf{u})\approx\mathbf{f}(z)\cdot\mathbf{u}, \tag{17}$$

$$\overline{f_i(z)f_j(z')}=\gamma\delta(z-z')\delta_{ij}. \tag{18}$$

The right-hand side of Eq. (17) being linear in $\mathbf{u}$ this leads to a Gaussian distribution of the displacements $\mathbf{u}$. Together with the dispersive elastic part we obtain at low temperatures,

$$\overline{\langle u\rangle^2}(L)\simeq 2\int_{1/L}^{1/d}\frac{dq}{2\pi}\frac{\gamma}{\varepsilon_l(q)^2q^4}\simeq\begin{cases} d<L<\varepsilon\lambda_{ab}: & \dfrac{\gamma}{(\varepsilon_0\varepsilon^2)^2}L^3 \\ L_d<L<\lambda_{ab}: & \overline{\langle u\rangle^2}(L_d)\simeq\dfrac{\gamma}{\varepsilon_l(q_d)^2}L_d^3 \\ L>\lambda_{ab}: & \dfrac{\gamma}{\varepsilon_0^2}L^3+\dfrac{\gamma}{\varepsilon_l(q_d)^2}L_d^3. \end{cases} \tag{19}$$

Up to numerical prefactors this result holds for all n. For $L=d$, only the Fourier mode with the largest wave vector $q=1/d$ contributes, and we cross over to the pinning of pointlike pancake vortices with only one degree of freedom, which will be discussed in Sec. IV B in detail. As for thermal fluctuations, we find that $\overline{\langle u\rangle^2}(L)$ is essentially *independent* of L for scales $L_d<L<\lambda_{ab}$ where the weak electromagnetic coupling dominates resulting in a plateau in the pinning-induced fluctuations $\overline{\langle u\rangle^2}(L)$ over a certain range of length scales. The roughness exponent for dispersion relations $\varepsilon_l(q)\propto q^{-\omega}$ is $\zeta_{RF}=(3-2\omega)/2$ and thus negative for $\omega>3/2$ such as the electromagnetic coupling with $\omega=2$. Again, one concludes that self-affinity is lost for $\omega>3/2$, which manifests itself in the last line of Eq. (19) that can be written as

$$\overline{\langle u\rangle^2}(L)\simeq\overline{\langle u\rangle_{q<\lambda}^2}(L)+\overline{\langle u\rangle^2}(L_d)\simeq\overline{\langle u\rangle^2}(L_d)\left[\left(\frac{L}{\tilde{L}_c}\right)^3+1\right] \tag{20}$$

in complete analogy to formula (10). The short-scale fluctuations are bigger on scales $L_d<L<\tilde{L}_c$ where

$$\tilde{L}_c\simeq L_d\left(\frac{\varepsilon_0}{\varepsilon_l(q_d)}\right)^{2/3}\simeq\frac{\lambda_{ab}^{4/3}}{L_d^{1/3}}\simeq\frac{\lambda_{ab}}{\max\{\varepsilon_d^{1/3},\varepsilon^{1/3}\}}. \tag{21}$$

Analogously to thermal fluctuations, $L_d<L<\tilde{L}_c$ thus specifies the extent of the plateau in the quenched displacements. The *pinning plateau length* $\tilde{L}_c$ also plays the role of an effective collective pinning length as long as $L_c<\tilde{L}_c$ as we will see below, cf. Eq. (36).

From Eq. (19) we can obtain the low-temperature collective pinning length for the case of a strong Josephson coupling $\varepsilon\lambda_{ab}>d$ using its definition $\overline{\langle u\rangle^2}(L_c)=\xi_{ab}^2$:

$$L_c\simeq\begin{cases} \delta_d=1: & d \\ \delta>\delta_{\varepsilon\lambda},\ \ 1>\delta_d: & L_{c,\varepsilon}=\varepsilon\xi_{ab}\left(\dfrac{\delta}{\varepsilon}\right)^{-1/3} \\ \delta=\delta_{\varepsilon\lambda}^+: & \varepsilon\lambda_{ab} \\ \delta=\delta_{\varepsilon\lambda}^-: & \tilde{L}_c\simeq\dfrac{\lambda_{ab}}{\varepsilon^{1/3}} \\ \delta\ll\delta_{\varepsilon\lambda}: & L_{c,i}=\xi_{ab}\delta^{-1/3}=\varepsilon^{-4/3}L_{c,\varepsilon} \end{cases} \tag{22}$$

[note that $\varepsilon_l(q_d)\simeq\varepsilon_l(1/d)\simeq\varepsilon_0\varepsilon^2$ for $\varepsilon\lambda_{ab}>d$ such that $\delta_d=(\delta/\varepsilon)(d/\varepsilon\xi_{ab})^3$]. $\delta=\delta_{\varepsilon\lambda}=\varepsilon\kappa^{-3}$ is the characteristic disorder strength at which $L_c=\varepsilon\lambda_{ab}$ and $\delta_d=1$ or $\delta=\varepsilon^4(\xi_{ab}/d)^3=\delta_{\varepsilon\lambda}(\varepsilon/\varepsilon_d)^3$ the required (higher) disorder strength for $L_c=d$. Within weak collective pinning theory we have to restrict ourselves to the regime $\delta_d<1$ in order to have $L_c>d$; at larger disorders pointlike pancake vortices are strongly pinned, which requires a different description, see Sec. IV B.

$L_{c,\varepsilon}$ is the usual result for the collective pinning length in an anisotropic superconductor as we find it if the Josephson coupling dominates on small scales, whereas $L_{c,i}$ is the isotropic result which we recover in the local limit on large scales due to the electromagnetic coupling. Because the displacements $\overline{\langle u\rangle^2}$ are essentially constant over the range $\varepsilon\lambda_{ab}<L<\tilde{L}_c$ up to the pinning plateau length $\tilde{L}_c$, the pin-

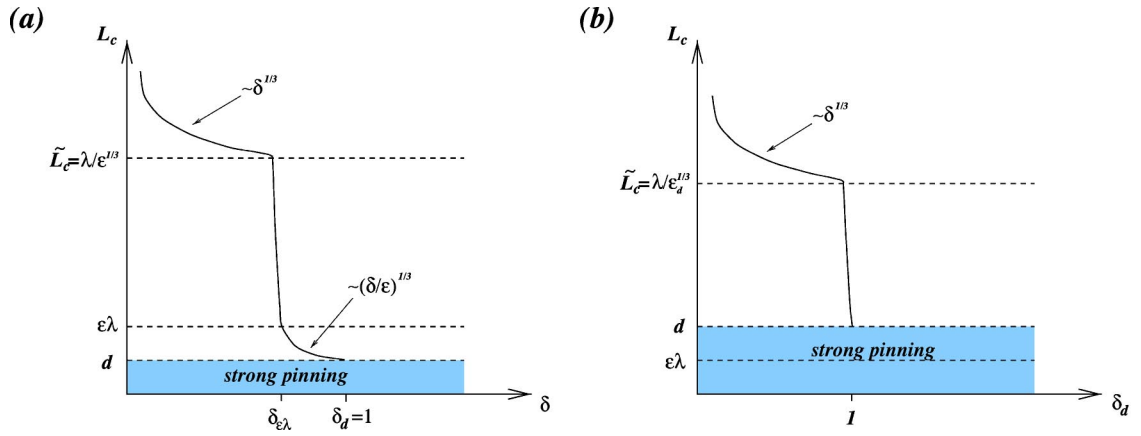

FIG. 1. Schematic plot of the disorder dependence of the collective pinning length L_c (a) for strong Josephson coupling $\varepsilon\lambda_{ab}>d$ according to Eq. (22) and (b) for weak Josephson coupling $d>\varepsilon\lambda_{ab}$ according to Eq. (23). For $L_c<d$ or $\delta_d>1$ strong pinning of pointlike pancake vortices sets in.

ning length jumps at $\delta=\delta_{\varepsilon\lambda}$ from $L_c=\varepsilon\lambda_{ab}$ to $L_c\simeq\tilde{L}_c$ upon weakening the disorder slightly. These results are illustrated in Fig. 1(a).

For a weak Josephson coupling $d>\varepsilon\lambda_{ab}$ it is more convenient to use the parameter δ_d for the disorder strength. Again restricting ourselves to $\delta_d<1$ we find in analogy to formula (22),

$$L_c\simeq\begin{cases}\delta_d=1: & d\\ \delta_d=1^-: & \tilde{L}_c\simeq\dfrac{\lambda_{ab}}{\varepsilon_d^{1/3}}\\ \delta_d\ll 1: & L_{c,i}=\xi_{ab}\delta^{-1/3}\\ & \simeq d\varepsilon_d^{-4/3}\delta_d^{-1/3}\simeq\tilde{L}_c\delta_d^{-1/3}\end{cases}\tag{23}$$

[note that $\varepsilon_l(q_d)=\varepsilon_l(1/d)\simeq\varepsilon_0\varepsilon_d^2$ for $d>\varepsilon\lambda_{ab}$]. In particular, we also have a jump from $L_c=d$ at $\delta_d=1$ to the pinning plateau length $L_c\simeq\tilde{L}_c$ upon weakening the disorder slightly, because the displacements $\overline{\langle u\rangle^2}$ are constant over the range $d<L<\tilde{L}_c$, see Fig. 1(b).

For weak collective pinning when $L_c>d$ the result (19) for the mean-square vortex displacements remains valid down to the shortest scale $L=d$ where it crosses over to corresponding *perturbative* results for the pinning of single-pancake vortices [see Eq. (31)]. For $L_c<d$, on the other hand, we have to consider strong pinning of single-pancake vortices which requires a nonperturbative treatment.

B. Strong pinning of pancake vortices

On the smallest scale in a layered superconductor $L=d$ we can no longer discuss deformations of an elastic vortex line of length L. Rather we have to consider the relative displacements $\mathbf{u}=\mathbf{u}[(l+1)d]-\mathbf{u}(ld)$ between single-*pancake segments* of the vortex line in two neighboring layers $l+1$ and l and discuss the pinning of single-pancake vortices.[9,19,20] This becomes particularly interesting as soon as $\delta_d>1$ where we formally find $L_c<d$ and enter a regime where pinning is no longer a small perturbation but pointlike pancake vortices are strongly pinned at low temperatures.

The problem of pancake vortex pinning is equivalent to that of a single-point particle (i.e., a short line segment with $L=d$) with n-component displacement $\mathbf{u}$ in a disorder potential $V_d(\mathbf{u})=dV(0,\mathbf{u})$ and a harmonic potential due to the coupling to the pancakes in adjacent layers. The Hamiltonian (1) for the relative pancake displacements becomes

$$\mathcal{H}_d=\frac{1}{2d}\varepsilon_l(1/d)\mathbf{u}^2+V_d(\mathbf{u}),\tag{24}$$

with $\varepsilon_l(1/d)\simeq\varepsilon_0(\varepsilon^2+\varepsilon_d^2)$ from Eq. (2). Note that we have neglected some logarithmic corrections in the Hamiltonian (24) which come from the additional u dependence of ε_l in the electromagnetic part in Eq. (2). Corrections due to these terms are generally small,[9,19,20] and they will be neglected in the following. The disorder potential $V_d(\mathbf{u})$ has a Gaussian distribution, zero mean, and short-range correlations:

$$\overline{V_d(\mathbf{u})V_d(\mathbf{u}')}=\frac{U_p^2}{\sqrt{2\pi}^n}\exp\left(-\frac{(\mathbf{u}-\mathbf{u}')^2}{2\xi_{ab}^2}\right)\approx U_p^2\xi_{ab}^n\delta_{\xi_{ab}}(\mathbf{u}-\mathbf{u}').\tag{25}$$

Then the distribution of realizations $V_d(\mathbf{u})$ is a product $P[V_d(\mathbf{u})]=\Pi_{\mathbf{u}}p(V_d(u))$ over independent distributions

$$p(E)=\frac{1}{\sqrt{2\pi}U_p}\exp\left(-\frac{1}{2}\frac{E^2}{U_p^2}\right).\tag{26}$$

The strong pinning ($\delta_d>1$) problem has been studied for $n=1$ by Imry-Ma arguments and a replica variational calculation.[21] Imry-Ma arguments have also been used for the case $n=2$ in Refs. 9, 19, and 20. At low temperatures a vortex with displacement u can explore $\mathcal{N}=u^2/\xi_{ab}^2$ pinning sites with statistically independent disorder configurations, see Fig. 2. Doing so it can gain a pinning energy $E_{\rm pin}(u)\simeq-U_p\ln^{1/2}(u^2/\xi^2)$ that can be determined from the condition $\mathcal{N}\int_{-\infty}^{E_{\rm pin}(u)}dEp(E)\sim 1$. In the Imry-Ma argument the total

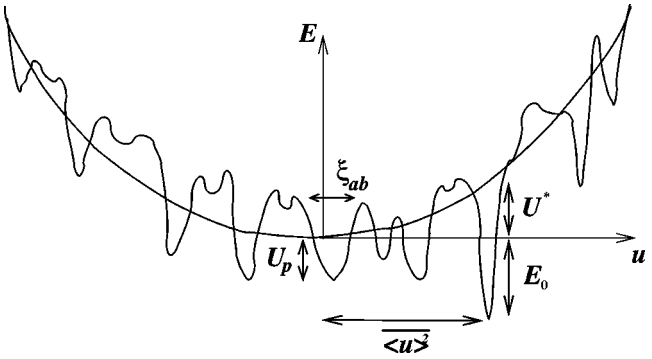

FIG. 2. Schematic plot of the energy (24), the sum of a harmonic potential and the disorder energy. The ground-state energy is E_0, typical elastic barriers are of size U_*.

energy $E(u)=E_{\rm pin}(u)+(1/2d)\varepsilon_l(1/d)u^2$ is minimized. The optimal disorder-induced displacement fluctuation u in the ground state is

$$u^2 \simeq \frac{dU_p}{\varepsilon_l(1/d)} \ln^{-1/2}\left(\frac{u}{\xi}\right). \tag{27}$$

Solving the last equation iteratively yields

$$\overline{\langle u\rangle^2} \simeq \xi_{ab}^2 \delta_d^{1/2} \ln^{-1/2}\delta_d . \tag{28}$$

The corresponding ground-state energy $E_0 \simeq E_{\rm pin}(u)$ is

$$E_0 \simeq -U_p \ln^{1/2}\delta_d , \tag{29}$$

whereas the typical elastic energy sets an energy scale $U^* \simeq (1/2d)\varepsilon_l(1/d)u^2$

$$U^* \simeq U_p \ln^{-1/2}\delta_d , \tag{30}$$

which is the typical size of elastic energy barriers between different metastable states as shown in Fig. 2.

Equation (28) is a nonperturbative result which holds for $\overline{\langle u\rangle^2} > \xi_{ab}^2$, which is exactly the condition $\delta_d > 1$ for strong pinning. Otherwise perturbation theory applies and we can expand the random potential $V_d(\mathbf{u})$ to linear order in $\mathbf{u}$ to obtain random forces acting on the pancake vortex. Then one finds

$$\overline{\langle u\rangle^2}_{RF} \simeq \xi_{ab}^2 \delta_d \tag{31}$$

which is the RF result for weakly pinned pancake vortices; for $L=d$, the results (31) and (19) coincide. $\overline{\langle u\rangle^2}_{RF} < \xi_{ab}^2$ implies that $L_c > d$ such that we cross over to the weak collective pinning of lines. From Eqs. (28) and (31) it follows that the crossover happens at $\delta_d = 1$ where we thus have $L_c \simeq d$. This is consistent with our findings (22) and (23).

In the RF treatment we neglect the competition of different energy barriers with almost degenerate pinning energies for the vortex position and consider only one valley the position of which is fluctuating from sample to sample. The typical pinning force is U_p/ξ_{ab} from the variation of the pinning energy U_p over the distance ξ_{ab} of disorder correlations.

C. Pinning in the random manifold regime

So far we have not considered the pinning-induced deformations of the vortex segment of length L on scales exceeding the Larkin length, i.e., $L > L_c$ for weak pinning or scales exceeding the layer spacing, i.e., $L > d$ for strong pinning. On these length scales, where displacements fulfill $\overline{\langle u\rangle^2}(L) > \xi_{ab}^2$, an expansion of the disorder potential in the displacements resulting in random forces does no longer hold, and we have to take into account the non-Gaussian distribution of pinning energies. Within this so-called RM regime no exact calculation is possible. A Flory argument can estimate the fluctuations by optimizing the free energy of fluctuations on a *single* length scale L. For a stiffness with dispersion relation $\varepsilon_l(q) \propto q^{-\omega}$ the typical elastic energy of the line $E_{el} \sim u^2 L^{-1+\omega}$, whereas the pinning energy that can be gained on the length L is $E_{\rm pin} \sim (L u^{-n})^{1/2}$. Optimizing $(E_{el} + E_{\rm pin})/L$ with respect to u gives $\overline{\langle u\rangle^2}(L) \sim L^{2(3-2\omega)/(4+n)}$, i.e., a roughness exponent $\zeta_{RM} = 3(1-2\omega/3)/(4+n)$. For $\omega = 0$ it is known that the estimate $\zeta_{RM} = (3+n)/2(2+n)$ improves on the Flory argument.[17,18] To interpolate to this $\omega = 0$ result, we suggest an estimate $\zeta_{RM} = (3+n)(1-2\omega/3)/2(2+n)$ for general ω on this phenomenological basis.

As long as $\omega < 3/2$ the vortex line is self-affine, and we can find the displacement fluctuations by normalizing the scaling relation $\overline{\langle u\rangle^2}(L) = L^{2\zeta_{RM}}$ appropriately. This applies to the nondispersive ($\omega = 0$) short-scale regimes $L_c < L < \varepsilon\lambda_{ab}$ for weak pinning $L_c > d$ [and thus for a strong Josephson coupling $\varepsilon\lambda_{ab} > d$ only] or $d < L < \varepsilon\lambda_{ab}$ for strong pinning $L_c < d$ [for a weak Josephson coupling $d > \varepsilon\lambda_{ab}$ only]. Furthermore it applies on large length scales $L > L_c > \tilde{L}_c$ in the case of weak pinning. For weak pinning we normalize the scaling relation using $\overline{\langle u\rangle^2}(L_c) = \xi_{ab}^2$ and find

$$\overline{\langle u\rangle^2}(L) \simeq \xi_{ab}^2 \left(\frac{L}{L_c}\right)^{2\zeta_{RM}} \tag{32}$$

for $L_c < L < \varepsilon\lambda_{ab}$ and $L > L_c > \tilde{L}_c$. For strong pinning, we normalize by employing the result (28) for $\overline{\langle u\rangle^2}(d)$, and we find

$$\overline{\langle u\rangle^2}(L) \simeq \overline{\langle u\rangle^2}(d) \left(\frac{L}{d}\right)^{2\zeta_{RM}} \tag{33}$$

for $d < L < \varepsilon\lambda_{ab}$.

However, ζ_{RM} becomes formally negative for all $\omega > 3/2$ such that an electromagnetic coupling (with $\omega = 2$) destroys the self-affine scaling properties of the line. This becomes relevant for $L > L_c$ if also $\tilde{L}_c > L_c$, which immediately implies the stronger inequality $\tilde{L}_c > L_d > L_c$ because of the jumps in the pinning length that we obtained in Eqs. (22) and (23). The resulting inequality $L_d > L_c$ applies for $\delta > \delta_{\varepsilon\lambda}$ if $\varepsilon\lambda_{ab} > d$ or $\delta_d > 1$ if $\varepsilon\lambda_{ab} < d$ (in the case of weak pinning $L_c > d$ the inequality can only be fulfilled for a strong Josephson coupling where $L_d = \varepsilon\lambda_{ab} > d$; for strong pinning $L_c < d$ the inequality is always fulfilled for a weak Josephson coupling where $L_d = d > \varepsilon\lambda_{ab}$). The cases of strong Josephson coupling $\varepsilon\lambda_{ab} > d$ and weak Josephson coupling d

$>\varepsilon\lambda_{ab}$ can be treated in a unified manner if we use corresponding definitions of the length scale L_d, see Eq. (4), and the pinning plateau length $\tilde{L}_c$, see Eq. (21). To find the displacements $\overline{\langle u\rangle^2}(L)$ in this part of the random manifold regime where dispersion is relevant we can argue in close analogy to thermal and random force fluctuations. First, we note that on scales $L_d<L<\lambda_{ab}$ the electromagnetic interaction leads to the decoupling of vortex elements such that $\overline{\langle u\rangle^2}(L)\simeq\overline{\langle u\rangle^2}(L_d)$ remains constant within this regime. On scales larger than λ_{ab}, we can formulate a coarse-grained model for the vortex line in terms of elastically coupled segments of length $\xi_{||}=\lambda_{ab}$, each of which explores an area $\xi_\perp^2=\overline{\langle u\rangle^2}(L_d)$ in the transversal direction. A given segment has to completely reoptimize its configuration if it is displaced by $u\sim\xi_\perp$. The typical pinning energy fluctuation ΔE_λ in such a reoptimization is obtained as the sum of energy fluctuations of the λ_{ab}/L_d independently adapting subsegments:

$$\Delta E_\lambda^2\simeq\frac{\lambda_{ab}}{L_d}[\varepsilon_l(q_d)\overline{\langle u\rangle^2}(L_d)L_d^{-1}]^2\simeq\varepsilon_l(q_d)^2\xi_{||}\xi_\perp^4L_d^{-3}. \tag{34}$$

Therefore on scales $L>\lambda_{ab}$ we can use a coarse-grained disorder potential $V_\lambda(z,\mathbf{u})$ with zero mean and a Gaussian distribution with

$$\overline{V_\lambda(z,\mathbf{u})V_\lambda(a',\mathbf{u}')}=\Delta E_\lambda^2\xi_{||}^{-1}\xi_\perp^2\delta_{\xi_{||}}(z-z')\delta_{\xi_\perp}(\mathbf{u}-\mathbf{u}'). \tag{35}$$

Thus the effective random force strength is $\gamma_\lambda=\Delta E_\lambda^2\xi_{||}^{-1}\xi_\perp^{-2}$. The coarse-grained dispersion-free stiffness for $L>\lambda_{ab}$ is the isotropic, local limit value $\varepsilon_\lambda\simeq\varepsilon_0$. Using such a coarse-grained model we read off an effective pinning length

$$\tilde{L}_c\simeq\xi_\perp^{2/3}\varepsilon_0^{2/3}\gamma_\lambda^{-1}\simeq L_d\left(\frac{\varepsilon_0}{\varepsilon_l(q_d)}\right)^{2/3}, \tag{36}$$

which is exactly the pinning plateau length found earlier in Eq. (21). In the coarse-grained model, the displacements for $L>\tilde{L}_c$ are

$$\overline{\langle u\rangle^2}(L)\simeq\overline{\langle u\rangle^2}(L_d)\left(\frac{L}{\tilde{L}_c}\right)^{2\zeta_{RM}}. \tag{37}$$

For scales $\lambda_{ab}<L<\tilde{L}_c$ it follows that $\overline{\langle u\rangle^2}(L)<\xi_\perp^2=\overline{\langle u\rangle^2}(L_d)$ such that short-scale fluctuations still dominate for these length scales. Hence the plateau is also present in the RM regime, and we obtain in complete analogy to formula (20),

$$\overline{\langle u\rangle^2}(L)\simeq\overline{\langle u\rangle^2}(L_d)\left[\left(\frac{L}{\tilde{L}_c}\right)^{\zeta_{RM}}+1\right], \tag{38}$$

also for the RM regime $L>L_c$ for the case $\tilde{L}_c>L_d>L_c$. This completes our analysis of pinning-induced fluctuations for weakly pinned vortex lines.

V. THERMAL DEPINNING

Thermal fluctuations weaken the pinning by averaging over thermally accessible configurations, which can lead to thermal depinning. For a pinned d-dimensional elastic manifold, thermal depinning is a phase transition from a thermally rough phase with $\zeta=1/2$ to a disorder roughened phase with a *bigger* $\zeta>1/2$ for $d<2n/(2+n)$,[3] i.e., for a vortex line with $d=1$ there is a phase transition for all $n>2$. For the physically relevant dimensions $n\leqslant 2$ there is no phase transition, and thermal fluctuations are irrelevant asymptotically, however, the crossover scale can become very large. This crossover scale is the pinning length $L_c(T)$ which starts to grow above a characteristic depinning temperature due to the weakening of the disorder by thermal fluctuations. In the marginal case $n=2$, the growth of $L_c(T)$ above the depinning temperature is exponential. For a pointlike pancake vortex with $d=0$, there is no phase transition in the thermodynamic sense possible but there is a crossover from the low-temperature result (28) of the Imry-Ma argument to a high-temperature regime where the RF result (31) holds.[21] In addition, there will be a crossover from strong pinning of pointlike pancake vortices to weak pinning of vortex lines if $L_c(T)<d$ at low temperatures but $L_c(T)>d$ at sufficiently high temperatures due to the increasing pinning length.[9] This interesting crossover for strong pinning will be studied in detail in Sec. V B; in the following section we focus on thermal depinning for weak collective pinning, i.e., $L_c(0)>d$.

A. Thermal depinning for weak pinning

In the presence of thermal fluctuations, the displacement has two parts $\mathbf{u}=\mathbf{u}_p+\mathbf{u}_{th}$ in the notation of Ref. 1. The part $\mathbf{u}_p$ is due to pinning and does not average to zero upon performing the thermal average: $\mathbf{u}_p=\langle\mathbf{u}\rangle$. The part $\mathbf{u}_{th}=\mathbf{u}-\langle\mathbf{u}\rangle$ describes thermal fluctuations around the pinning part. In weak collective pinning theory it is always assumed that the thermal averages over fluctuations of u_{th} can be performed just with the elastic Hamiltonian as in the absence of disorder; thus it is assumed that thermal averages are Gaussian. By exploiting a tilt symmetry of the system[22] one can establish that $\overline{\langle u_{th}^2\rangle}$ is indeed unchanged by the disorder,

$$\overline{\langle u_{th}^2\rangle}=\overline{\langle u^2\rangle}-\overline{\langle u\rangle^2}=\langle u^2\rangle_T, \tag{39}$$

but the distribution of u_{th} is non-Gaussian on large scales.[23] Both findings can also be put in the language of a replica variational calculation along the lines of Refs. 21 and 24, where an instability with respect to replica symmetry-breaking (RSB) signals that u_{th} is not Gaussian distributed. Only the replica symmetric solution, which corresponds to a self-consistent RF approximation, has both displacements u_{th} and u_p Gaussian distributed. Therefore, only in the RF regime on scales $L<L_c(T)$ it can be justified to thermally average as in the absence of disorder, which is used to calculate $L_c(T)$ within the weak collective pinning theory.

To obtain $L_c(T)$ also for a dispersive line stiffness, we follow the dynamic approach that is also employed in Ref. 1, in which the dynamic response to random forces is taken into

account using an overdamped dynamics with a vortex line viscosity η_l. This allows one to write thermal averages $\langle u^2\rangle_T(t) \simeq \frac{1}{2}\langle [u(t)-u(0)]^2\rangle_t$ for a dispersive line stiffness in the absence of the pinning potential as

$$\langle u^2\rangle_T(t) \simeq T\int \frac{dq}{2\pi}\frac{1}{\varepsilon_l(q)q^2}\{1-\exp[-\varepsilon_l(q)q^2 t/\eta_l]\} \simeq 2\int_{q(t)}^{\infty}\frac{dq}{2\pi}\frac{T}{\varepsilon_l(q)q^2}, \tag{40}$$

which converges to the result (9) for $t\to\infty$ but at finite times, the large-scale cutoff is provided by $1/q(t)$, defined as solution to the equation $\varepsilon_l(q(t))q(t)^2=\eta_l/t$. Dynamic random forces are obtained by expanding the potential $V[z,\mathbf{u}_p(t)+\mathbf{u}_{th}(t)]$ of Eq. (13) in $\mathbf{u}_p(t)$ about $\mathbf{u}_p=0$. In order to calculate $\overline{\langle u(q)\rangle\langle u(q')\rangle}=G_{RF}(q)2\pi\delta(q+q')$, we perform the thermal averages $\langle u_{th}^2\rangle_T(t)$ using the result (40). This gives

$$\begin{aligned} G_{RF}(q) &\simeq \frac{\gamma}{\varepsilon_l(q)q^2}\int_0^{\infty}\frac{dt}{\eta_l}e^{-\varepsilon_l(q)q^2t/\eta_l}\int\frac{d^2K}{(2\pi)^2}K^2 \times e^{-K^2[\xi_{ab}^2+\langle u_{th}^2\rangle_T(t)]} \\ &\simeq \frac{\gamma}{\varepsilon_l(q)q^2}\int_0^{\infty}\frac{dt}{\eta_l}e^{-\varepsilon_l(q)q^2t/\eta_l}\frac{\xi_{ab}^4}{[\xi_{ab}^2+\langle u_{th}^2\rangle_T(t)]^2} \\ &\simeq \frac{\gamma}{\varepsilon_l(q)q^2}\int_q^{\infty}dq_1\frac{1}{\varepsilon_l(q_1)q_1^3} \times\frac{\xi_{ab}^4}{\left\{\xi_{ab}^2+2\int_{q_1}^{\infty}(dq_2/2\pi)[T/\varepsilon_l(q_2)q_2^2]\right\}^2}, \end{aligned} \tag{41}$$

where we replaced the exponential decay with t by cutting off the t integration for long times at $t(q)=\eta_l/\varepsilon_l(q)q^2$, used the relation $t=t(q)$ to switch back to integration variables q, and finally set $(d/dq)(\varepsilon_l(q)q^2)\simeq\varepsilon_l(q)q$ to a good approximation. The advantage of the dynamical approach is to generate the proper hierarchy of IR regularizations in the q integrals in Eq. (41). Performing the integrals and Fourier transforming finally gives the result

$$\overline{\langle u\rangle^2}(L) \simeq 2\int_{1/L}^{\infty}\frac{dq}{2\pi}\frac{\gamma}{\varepsilon_l(q)q^2}\int_0^{1/q}dl\frac{l}{\varepsilon_l(1/l)}\frac{\xi_{ab}^4}{[\xi_{ab}^2+\langle u^2\rangle_T(l)]^2}$$

$$\simeq\begin{cases} d<L<\varepsilon\lambda_{ab}: & \overline{\langle u\rangle_{T=0}^2}(L)\left(\dfrac{\xi_{ab}^2}{\xi_{ab}^2+\langle u^2\rangle_T(L)}\right)^2\ln\left(e+\dfrac{\langle u^2\rangle_T(L)}{\xi_{ab}^2}\right) \\ d<\varepsilon\lambda_{ab}<L<\lambda_{ab}: & \overline{\langle u\rangle_{T=0}^2}(\varepsilon\lambda_{ab})\left(\dfrac{\xi_{ab}^2}{\xi_{ab}^2+\langle u^2\rangle_T(\varepsilon\lambda_{ab})}\right)^2\ln\left(e+\dfrac{\langle u^2\rangle_T(\varepsilon\lambda_{ab})}{\xi_{ab}^2}\right) \\ \varepsilon\lambda_{ab}<d<L<\lambda_{ab}: & \overline{\langle u\rangle_{T=0}^2}(d)\left(\dfrac{\xi_{ab}^2}{\xi_{ab}^2+\langle u^2\rangle_T(d)}\right)^2 \\ \lambda_{ab}<L<\tilde{L}: & \overline{\langle u\rangle_{T=0}^2}(L)\left(\dfrac{\xi_{ab}^2}{\xi_{ab}^2+\langle u^2\rangle_T(L_d)}\right)^2 \\ \tilde{L}<L: & \overline{\langle u\rangle_{T=0}^2}(L)\left(\dfrac{\xi_{ab}^2}{\xi_{ab}^2+\langle u^2\rangle_T(L)}\right)^2\ln\left(e+\dfrac{\langle u^2\rangle_T(L)}{\xi_{ab}^2+\langle u^2\rangle_T(L_d)}\right), \end{cases} \tag{42}$$

which takes into account all possible cases with regard to the vortex length L relative to the length scales $\varepsilon\lambda_{ab}$ and d introduced by the dispersion and the thermal plateau length $\tilde{L}$. As becomes clear from the structure of the expressions, the thermal smoothing of the disorder potential as well as the random-force-induced displacements themselves are affected by the electromagnetic coupling. Within the plateau regime for thermal fluctuations, $L_d<L<\tilde{L}$, the thermal smoothing essentially comes from fluctuations on the scale L_d because line elements effectively decouple. The effects on disorder-induced fluctuations themselves manifest in the first factor giving the low-temperature result $\overline{\langle u\rangle_{T=0}^2}(L)$ as calculated in Eq. (19). As we saw above, these fluctuations stay constant in the plateau regime $L_d<L<\tilde{L}_c$, see Eq. (20). In Sec. V B, it will become clear that the above result (42) is only correct if we can treat pinning on all length scales by weak collective pinning theory. This becomes wrong as soon as $\delta_d>1$ or $L_c(0)<d$ when we have strong pinning of pancake vortices. Then all thermal smoothing terms $\langle u^2\rangle_T(L)$ in Eq. (42) have to be replaced by the number $N(T,L)$ of states accessible by

thermal fluctuations of vortex segments of length L. This number will be estimated for the strong pinning case in Sec. V B, see Eq. (69).

It is evident that the rich behavior of the displacement fluctuations (20) for a dispersive line stiffness will also lead to interesting features for the pinning length $L_c(T)$. Taking into account the thermal smoothing of the pinning potential, the perturbative approach is valid as long as $\overline{\langle u\rangle^2}(L)<\xi_{ab}^2+\langle u^2\rangle_T(L)$ because thermal fluctuations increase the disorder correlation length to an effective value $\xi_{ab}^2+\langle u^2\rangle_T(L)$, see Eq. (41). Therefore, the temperature-dependent pinning length $L_c(T)$ is obtained by the condition $\overline{\langle u\rangle^2}(L_c(T))=\xi_{ab}^2+\langle u^2\rangle_T(L_c(T))$, which can be evaluated using Eqs. (9), (19), and (42).

Depending on the size of the $T=0$ pinning length (22) or (23) in comparison to the scales L_d and $\tilde{L}$, the thermal depinning will happen at different characteristic temperatures such that we have to distinguish three cases within the weak pinning regime

$$\text{(i) large disorder } L_c(0)<L_d \tag{43}$$

[for weak pinning we only consider $L_c(0)>d$ in order to have weak collective pinning of lines at $T=0$ such that the regime (i) becomes $d<L_c(0)<\varepsilon\lambda_{ab}$ and is present *only* for a strong Josephson coupling; strong pinning of pancakes will be discussed in the following section],

$$\text{(ii) intermediate disorder } \tilde{L}_c<L_c(0)<\tilde{L} \tag{44}$$

[remember that $L_c(0)$ jumps from L_d to the pinning plateau length $\tilde{L}_c$ and essentially does not take on values in between, see Eq. (22)], and

$$\text{(iii) very weak disorder } L_c(0)>\tilde{L}. \tag{45}$$

We will use the abbreviations (i), (ii), (iii) throughout the whole paper to denote the corresponding cases.

For a strong Josephson coupling $\varepsilon\lambda_{ab}>d$, we find

$$\text{(i):}L_c(T)\simeq\begin{cases} T<T_{dp,\varepsilon}: & L_{c,\varepsilon}\\ T_{dp,\varepsilon}<T<T_{\varepsilon\lambda}: & L_{c,\varepsilon}\dfrac{T_{dp,\varepsilon}}{T}e^{(T/T_{dp,\varepsilon})^3}\\ T=T_{\varepsilon\lambda}^-: & \varepsilon\lambda_{ab}\\ T=T_{\varepsilon\lambda}^+: & \tilde{L}_c\simeq\dfrac{\lambda_{ab}}{\varepsilon^{1/3}}\simeq\tilde{L}\varepsilon^{2/3}\\ T_{\varepsilon\lambda}^+<T<T_{dp,i}: & \tilde{L}_c\dfrac{T}{T_{\varepsilon\lambda}}\simeq\tilde{L}\dfrac{T}{T_{dp,i}}\\ T>T_{dp,i}: & \tilde{L}e^{(T/T_{dp,i})^3}, \end{cases} \tag{46a}$$

$$\text{(ii):}L_c(T)\simeq\begin{cases} T<T_{dp,\varepsilon\lambda}: & L_{c,i}\\ T_{dp,\varepsilon\lambda}<T<T_{dp,i}: & L_{c,i}\dfrac{T}{T_{dp,\varepsilon\lambda}}\simeq\tilde{L}\dfrac{T}{T_{dp,i}}\\ T>T_{dp,i}: & \tilde{L}e^{(T/T_{dp,i})^3} \end{cases} \tag{46b}$$

$$\text{(iii):}\quad L_c(T)\simeq\begin{cases} T<T_{dp,i}: & L_{c,i}\\ T_{dp,i}<T<T_{dp,\varepsilon\lambda}: & L_{c,i}\dfrac{T_{dp,i}}{T}e^{(T/T_{dp,i})^3}\\ T>T_{dp,\varepsilon\lambda}: & \tilde{L}e^{(T/T_{dp,i})^3}, \end{cases} \tag{46c}$$

with characteristic temperatures

$$T_{dp,\varepsilon}\simeq\varepsilon^{2/3}\varepsilon_0^{1/3}\xi_{ab}^{4/3}\gamma^{1/3}=\varepsilon\varepsilon_0\xi_{ab}\left(\frac{\delta}{\varepsilon}\right)^{1/3}, \tag{47}$$

$$\begin{aligned} T_{\varepsilon\lambda}&\simeq T_{dp,\varepsilon}\ln^{1/3}\left(\frac{T_{dp,\varepsilon}}{T_{dp,\varepsilon\lambda}}\right)-T_{dp,\varepsilon\lambda}\\ &\simeq T_{dp,\varepsilon}\left\{\ln^{1/3}\left[\left(\frac{\delta}{\delta_{\varepsilon\lambda}}\right)^{1/3}\right]-\left(\frac{\delta_{\varepsilon\lambda}}{\delta}\right)^{1/3}\right\}, \end{aligned} \tag{48}$$

$$T_{dp,\varepsilon\lambda}\simeq\varepsilon_0\xi_{ab}\frac{\varepsilon}{\kappa}\simeq T_{dp,\varepsilon}\left(\frac{\delta_{\varepsilon\lambda}}{\delta}\right)^{1/3}, \tag{49}$$

$$T_{dp,i}\simeq\varepsilon_0^{1/3}\xi_{ab}^{4/3}\gamma^{1/3}=\varepsilon_0\xi_{ab}\delta^{1/3}=\varepsilon^{-2/3}T_{dp,\varepsilon}. \tag{50}$$

The different regimes in the temperature dependence of the pinning length $L_c(T)$ for strong Josephson coupling are illustrated in Fig. 3(a). For large disorder (i), i.e., short scales $L_c(0)<\varepsilon\lambda_{ab}$ or $\delta>\delta_{\varepsilon\lambda}$ [but $L_c(0)>d$ or $\delta_d<1$], Eq. (46) gives the usual anisotropic result with an exponentially increasing $L_c(T)$ above the *anisotropic depinning temperature* $T_{dp,\varepsilon}$.[1] This behavior will continue until $L_c(T)=\varepsilon\lambda_{ab}$, which defines the slightly higher temperature $T_{\varepsilon\lambda}$. Due to the electromagnetic coupling, the displacements $\overline{\langle u\rangle^2}(L)$ stay essentially constant on scales $\varepsilon\lambda_{ab}<L<\tilde{L}_c$ up to the pinning plateau length such that the pinning length jumps at the temperature $T_{\varepsilon\lambda}$ from $L_c=\varepsilon\lambda_{ab}$ to $L_c\simeq\tilde{L}_c$ upon a small temperature increase. In the range $\tilde{L}_c<L<\tilde{L}$ disorder-induced fluctuations start to increase again with L according to Eq. (20) but the thermal fluctuations responsible for the weakening of the disorder are still essentially constant due to the electromagnetic interactions. This leads to a less effective smoothing and the pinning length grows only linearly with T. Finally, on scales $L>\tilde{L}$, both thermal and disorder-induced fluctuations increase with L. Because the stiffness takes on the isotropic value $\varepsilon_l\simeq\varepsilon_0$ from the local limit of the electromagnetic coupling, the characteristic depinning temperature is the isotropic $T_{dp,i}$. But also for $T>T_{dp,i}$ the temperature dependence of $L_c(T)$ is slightly different from the usual isotropic behavior because the additional log divergence in the last line of Eq. (42) is cutoff at small scales by the thermal plateau length $\tilde{L}$ due to the small-scale thermal fluctuations favored by the electromagnetic coupling.

For intermediate disorder (ii), $\lambda_{ab}/\varepsilon^{1/3}<L_c(0)<\lambda_{ab}/\varepsilon$, the *depinning temperature for the scale* $\varepsilon\lambda_{ab}$ called $T_{dp,\varepsilon\lambda}$ is most relevant. [Note that due to the dispersion of the stiffness, $T_{dp,\varepsilon\lambda}$ is also the depinning temperature for the thermal plateau length $\tilde{L}$, cf. Eq. (10)]. Starting from the isotropic value $L_{c,i}$ at low temperatures, the depinning is driven by short-scale thermal fluctuations on the scale $\varepsilon\lambda_{ab}$. (For in-

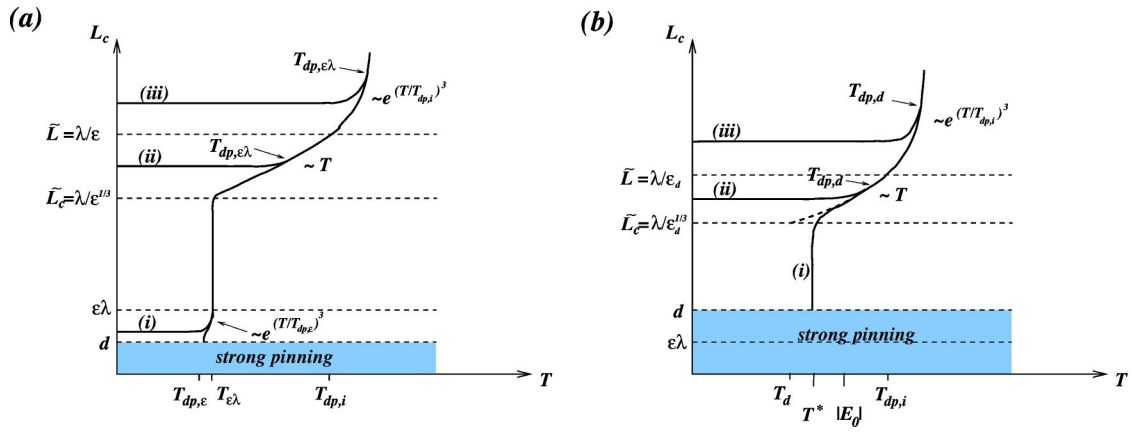

FIG. 3. Schematic plot of the temperature dependence of the collective pinning length L_c (a) for strong Josephson coupling $\varepsilon\lambda_{ab}>d$ (e.g., for YBCO) according to Eq. (46) and (b) for weak Josephson coupling $d>\varepsilon\lambda_{ab}$ (e.g., for BSCCO) according to Eq. (51). For $L_c<d$ strong pinning of pointlike pancake vortices sets in (shaded region). The corresponding curves for the case of strong pinning are also shown at the left and right; they emerge from the strong pinning regime at $T=T^*$ and are described by Eqs. (71) and (72).

termediate disorder, we have $T_{dp,\varepsilon\lambda}<T_{dp,i}$.) For weak disorder (iii), $L_c(0)>\lambda_{ab}/\varepsilon$, the thermal depinning is driven by thermal fluctuations on the scale of the isotropic Larkin length $L_{c,i}$ itself, and the relevant depinning temperature is the usual isotropic result $T_{dp,i}$. (For weak disorder, we have $T_{dp,i}<T_{dp,\varepsilon\lambda}$.)

For a weak Josephson coupling $d>\varepsilon\lambda_{ab}$, we can perform the same analysis and get analogous results. However, the case (i) of large disorder $L_c(0)<d$ or $\delta_d>1$ is peculiar because the condition puts us in the regime of strong pinning of pancakes, and only at temperatures high enough such that $L_c(T)>d$ we can get weak pinning of lines. This requires a theory for thermal depinning from strong pinning which we defer to the following Sec. V B. The basic differences to the case of strong Josephson coupling are the different definition of the thermal plateau length $\tilde{L}$, see Eq. (11), and in regimes (ii) and (iii) thermal depinning is now governed by fluctuations on the scale d instead of $\varepsilon\lambda_{ab}$ such that the corresponding temperature $T_{dp,d}$ is the relevant depinning temperature. As long as weak collective pinning theory applies and $L_c(T)>d$, we obtain

$$\text{(i):}\quad L_c(T)\simeq\begin{cases} T<T_{dp,i}: & \tilde{L}_c\dfrac{T}{T_d}\simeq\tilde{L}\dfrac{T}{T_{dp,i}} \\ T>T_{dp,i}: & \tilde{L}e^{(T/T_{dp,i})^3}, \end{cases} \tag{51a}$$

$$\text{(ii):}\quad L_c(T)\simeq\begin{cases} T<T_{dp,d}: & L_{c,i} \\ T_{dp,d}<T<T_{dp,i}: & L_{c,i}\dfrac{T}{T_{dp,d}}\simeq\tilde{L}\dfrac{T}{T_{dp,i}} \\ T>T_{dp,i}: & \tilde{L}e^{(T/T_{dp,i})^3}, \end{cases} \tag{51b}$$

$$\text{(iii):}\quad L_c(T)\simeq\begin{cases} T<T_{dp,i}: & L_{c,i} \\ T_{dp,i}<T<T_{dp,d}: & L_{c,i}\dfrac{T_{dp,i}}{T}\simeq\tilde{L}\dfrac{T}{T_{dp,i}} \\ T>T_{dp,d}: & \tilde{L}e^{(T/T_{dp,i})^3}, \end{cases} \tag{51c}$$

with characteristic temperatures

$$T_{dp,d}\simeq\varepsilon_l(1/d)\xi_{ab}^2/d=U_p\delta_d^{-1/2}, \tag{52}$$

$$T_d\simeq T_{dp,d}(\delta_d^{1/3}-1)=U_p(\delta_d^{-1/6}-\delta_d^{-1/2}), \tag{53}$$

$$T_{dp,i}\simeq\varepsilon_0^{1/3}\xi_{ab}^{4/3}\gamma^{1/3}=(\varepsilon_0\xi_{ab}^2/d)\varepsilon_d^{4/3}\delta_d^{1/3}. \tag{54}$$

Figure 3(b) shows the different regimes in the temperature dependence of the pinning length $L_c(T)$ for weak Josephson coupling. A detailed study of the case (i) of strong pinning will be presented in the following section, also for the case of strong Josephson coupling ($\varepsilon\lambda_{ab}>d$). In particular, we will clarify how $L_c(T)$ increases beyond d by thermal smoothing for the strong pinning situation $L_c(0)<d$. The discussion for the cases (ii) and (iii) of intermediate and very weak disorder carries through analogously to the previous discussion for strong Josephson coupling.

B. Thermal depinning from strong pinning

Now we address the thermal depinning of pancake vortices which are pinned on the scale $L=d$. The thermal depinning will be qualitatively different for weakly pinned pancake vortices with $\delta_d<1$ and strongly pinned pancake vortices with $\delta_d>1$ [or $L_c(0)<d$]. In particular, it has to be worked out how to cross over to the findings for weakly pinned lines on scales $L>d$ if the temperature becomes sufficiently high.

It is instructive to discuss first what happens if we naively assume that all thermal averages can be performed with the elastic part of the Hamiltonian as in the absence of disorder as it is justified in weak collective theory, i.e., for weakly pinned pancake vortices which have displacements (31) at low temperatures. Similar to vortex lines, this means that the range of the pinning forces is smeared out and we have to replace ξ_{ab}^2 by the effective vortex core area $\xi_{ab}^2+\langle u^2\rangle_T(d)$, cf. Eq. (41). With Gaussian thermal fluctuations of the vortex cores, we can define a thermally averaged pinning potential $\overline{V}_d$ by $\overline{V}_d(\langle u\rangle)=\langle V_d(\mathbf{u})\rangle$ which will again be

Gaussian distributed as in Eq. (25) but with a thermally weakened characteristic energy

$$\overline{U_p^2}(T)=U_p^2\frac{\xi_{ab}^2}{\xi_{ab}^2+\langle u^2\rangle_T(d)}\simeq\frac{U_p^2}{1+T/T_{dp,d}}. \tag{55}$$

This means $T_{dp,d}$ is the characteristic *depinning temperature for weakly pinned pancake vortices*. The Imry-Ma argument is made in the same way as at $T=0$ with a slightly lower number of statistically independent smeared pinning sites $N=u^2/(\xi_{ab}^2+\langle u^2\rangle_T)$, and we find for the optimal displacement

$$\overline{\langle u\rangle^2}\simeq\xi_{ab}^2\delta_d^{1/2}\left(1+\frac{T}{T_{dp,d}}\right)^{-1/2}\ln^{-1/2}\delta_d. \tag{56}$$

This result is expected to hold for $\overline{\langle u\rangle^2}>\xi_{ab}^2+\langle u^2\rangle_T$, otherwise perturbation or random force theory applies which gives with the same thermally weakened disorder potential,

$$\overline{\langle u\rangle^2}_{RF}\approx\xi_{ab}^2\delta_d\left(1+\frac{T}{T_{dp,d}}\right)^{-2} \tag{57}$$

[note that thermally averaged random forces are also Gaussian distributed but as *derivatives* of the potential, see Eq. (17), they have an additional factor $(1+T/T_{dp,d})^{-1}$ in their thermally weakened correlations (18) as compared to Eq. (55)].

At $T_d\simeq T_{dp,d}(\delta_d^{1/3}-1)$ we find $\overline{\langle u\rangle^2}\simeq\xi_{ab}^2\delta_d^{1/3}$ both with the Imry-Ma argument (56) and perturbation theory (57), moreover $\overline{\langle u\rangle^2}\simeq\langle u^2\rangle_T$, and both results cross exactly over to the line like weak pinning result (42) with $L=d$ as can be checked easily. Altogether this clearly suggests $L_c(T_d)\simeq d$ and a smooth crossover to weak collective pinning theory of lines on scales $L>d$. Though this scenario is consistent it turns out not to be correct because the thermal averages in Eq. (55) are performed as in the absence of disorder with a Gaussian distribution. This is essentially justified if disorder is a small perturbation but in the regime of strong pinning the relevant thermal fluctuations giving rise to the thermal smearing are non-Gaussian.[23] As a result formulas (56) and (57) are incorrect for the case $\delta_d>1$ of strongly pinned pancake vortices whereas our argumentation is justified for weakly pinned pancake vortices $\delta_d<1$ which are correctly described by formula (57).

The problem for the case of strongly pinned pancakes is clearly recognized if we generalize the replica variational calculation of Ref. 21 from $n=1$ to general n and apply it to the physical problem of pancake pinning with $n=2$ at hand. As usual in replica variational calculations, the perturbative RF result (57) is exactly what is found as the replica symmetric (RS) solution:

$$\frac{1}{n}\overline{\langle u^2\rangle}_{RS}=\frac{1}{n}\xi_{ab}^2\frac{T}{T_{dp,d}}+(2\pi)^{-n/2}\xi_{ab}^2\delta_d\left(1+\frac{T}{T_{dp,d}}\right)^{-1-n/2}, \tag{58}$$

$$T_{dp,d}=\frac{1}{2n}\varepsilon_l(1/d)\xi_{ab}^2/d. \tag{59}$$

Next, one checks for the stability of this RS solution with respect to RSB; the temperature below which the RS solution becomes locally unstable (which defines the so-called Almeida-Thouless line) turns out to be exactly the temperature T_d that we have identified above as the crossover temperature to linelike weak collective pinning. Within the replica variational approach we can specify numerical prefactors, and for $n=2$, we find

$$T_d=T_{dp,d}\left[\left(\frac{4}{\pi}\delta_d\right)^{1/3}-1\right]. \tag{60}$$

This instability temperature is identical to the temperature where the RS mean-square displacement $\overline{\langle u^2\rangle}_{RS}$ from Eq. (58) has a minimum as a function of T or where $\overline{\langle u\rangle^2}_{RS}\simeq\langle u^2\rangle_T$.

However, following Ref. 21 it can be shown that it is not the temperature T_d which marks the onset of glassy behavior. Rather, one finds that below a certain temperature T^* a one-step RSB solution becomes locally stable. In the limit $\delta_d\gg1$ of strong pinning the crossover temperature is

$$T^*=U^*=(2\pi)^{-n/4}U_p\ln^{-1/2}[n(2\pi)^{-n/4}\delta_d^{1/2}] \tag{61}$$

and $T^*\propto\delta_d^{1/2}$ is higher than $T_d\propto\delta_d^{1/3}$. In the same limit $\delta_d\gg1$ displacements and the variational free energy are

$$\frac{1}{n}\overline{\langle u^2\rangle}_{RSB}=(2\pi)^{-n/4}\xi_{ab}^2\delta_d^{1/2}\ln^{-1/2}[n(2\pi)^{-n/4}\delta_d^{1/2}]\times\left(1+\frac{T}{|E_0|}\right)^{-n/4}, \tag{62}$$

$$|F|=\tfrac{1}{2}(2\pi)^{-n/4}U_p\ln^{1/2}[n(2\pi)^{-n/4}\delta_d^{1/2}]. \tag{63}$$

The variational free energy $F\approx E_0$ is dominated by the ground-state energy at low temperatures.

Equation (62) describing the thermal depinning of a strongly pinned pancake vortex is the main result of this section and requires some further discussion. T^* is identical to the temperature where $\overline{\langle u^2\rangle}_{RSB}=\overline{\langle u^2\rangle}_{RS}$ or $\overline{\langle u\rangle^2}_{RSB}\simeq\langle u^2\rangle_T$ and the energy scale U^* from Eq. (30) that we identified as typical elastic energy barriers between different metastable energy minima for the pancake. As can be seen in Eq. (62), the characteristic depinning temperature in the one-step RSB solution is the ground-state energy $|E_0|$ of the $T=0$ problem. Note that formula (63) is identical to the result (29) from the Imry-Ma argument but specifies numerical prefactors. In particular, $|E_0|>T^*$ such that the disorder-induced fluctuations $\overline{\langle u^2\rangle}_{RSB}$ do not experience considerable thermal smoothing up to the temperature where the RSB solution becomes unstable. Thus the one-step RSB solution is essentially temperature independent and identical to the result (28) of the $T=0$ Imry-Ma argument in the whole temperature range $T<T^*$. This suggests that pancakes are strongly pinned in valleys of depth $\simeq|E_0|$, whereas thermal activation into energetically close valleys starts to occur at temperatures $\simeq T^*$ leading to the instability of the RSB solution. Therefore typical intervalley energy differences are indeed $U^*\simeq T^*$.

As already noted we have $T^*>T_d$ for strong pinning $\delta_d>1$. So the RSB solution is the only stable extremum of the free energy at low enough temperatures $T<T_d$ whereas the RS solution is the only stable extremum at high enough temperatures $T>T^*$. The situation is somewhat more complicated in the range $T_d<T<T^*$, where both solutions are locally stable but it can be shown that the RSB solution is the global energy minimum.[21] This is reminiscent of the ''competition'' that is induced by the fact that for $T>T_d$ the pinning should become linelike as suggested by the naive introductory argument but on the other hand, the individual pancake elements are still strongly pinned in valleys of depth $\simeq|E_0|$.

The results we obtained so far further suggest that within the small temperature range $T^*<T<|E_0|$ the strongly pinned pancakes will completely liberate from the valleys of depth $\simeq|E_0|$ and essentially all states become thermally accessible at temperatures $T\simeq|E_0|$. Then thermal fluctuations are only weakly affected by the strong pinning energy minima of the individual pancake segments such that a crossover to the weak collective pinning of lines as outlined in the preceding section takes place. For a vanishing Josephson coupling this crossover has been described as ''variable-range thermal smoothing'' in Ref. 9. The central quantity in the Imry-Ma argument presented for $T=0$ above is the number of accessible states N given a ground-state energy E_0. At $T=0$ we have

$$N(0)=\frac{\overline{\langle u^2\rangle}}{\xi_{ab}^2}\int_{-\infty}^{E_0}dEp(E), \tag{64}$$

where the ground-state energy fulfills $N(0)=1$ by definition. From our interpretation in terms of energy valleys of depth $\simeq|E_0|$ and intervalley energy differences $\simeq T^*$ we expect $N(T)$ to sharply increase in the temperature interval $T^*<T<|E_0|$. For $T>0$ there are two effects which increase $N(T)$. First, for $T>T^*$ we have $\langle u^2\rangle_T>\overline{\langle u\rangle^2}$, and the ''search'' or ''trapping'' area increases to $\overline{\langle u\rangle^2}+\langle u^2\rangle_T$. This is the dominant effect at high temperatures and reproduces the weak pinning theory results. Second, and more important for strong pinning at low temperatures, essentially all energies up to E_0+T can be probed by the pancake particle: Given a ground-state energy E_0 at $T=0$, the probability of occupying a pancake state of energy E at temperature T is given by $\exp[-(E-E_0)/T]/\{1+\exp[-(E-E_0)/T]\}$, which is reminiscent of a Fermi-like distribution as two pancakes repel and cannot occupy the same pinning site. Upon disorder averaging this gives for the number of accessible states at temperature T,

$$\begin{aligned}N(T)&=\frac{\overline{\langle u\rangle^2}+\langle u^2\rangle_T}{\xi_{ab}^2}\int_{-\infty}^{\infty}dEp(E)\frac{1}{1+\exp[(E-E_0)/T]}\approx\frac{\overline{\langle u\rangle^2}+\langle u^2\rangle_T}{\xi_{ab}^2}\int_{-\infty}^{E_0+T}dEp(E),\\&\simeq\begin{cases}T<T^*: & O(1)\\ T^*<T\ll|E_0|: & \left(1+\dfrac{T}{T^*}\right)\left(1+\dfrac{T}{|E_0|}\right)^{-1}\exp\left(c\dfrac{T}{T^*}-\dfrac{1}{2}\dfrac{T^2}{U_p^2}\right)\\ T>|E_0|: & \dfrac{T}{T_{dp,d}},\end{cases}\end{aligned} \tag{65}$$

where we used $N(0)=1$, $T^*=cU_p^2/|E_0|$ with a numerical constant $c=\frac{1}{2}(2\pi)^{-n/2}$ from Eqs. (63) and (61), and the approximation $\mathrm{erfc}(z)=1/\sqrt{\pi}\int_{-\infty}^{z}dxe^{-x^2}\approx 1/2\sqrt{\pi}|z|^{-1}e^{-z^2}$ for $z\ll-1$ if $T\ll|E_0|$, and $\frac{1}{2}<\mathrm{erfc}(z)<1$ if $T>|E_0|$. Taking only the leading terms of the result (65) and using $c=1$ in order to have a smooth crossover at $T\simeq|E_0|$ we obtain the approximate simplified expression

$$N(T)\simeq\left(1+\frac{T}{T^*}\right)\exp\left(\frac{T}{T^*}\right) \tag{66}$$

for $T<|E_0|$. An expression for $N(T)$ is at the heart of a theory of thermal smearing because it quantifies the number of states the disorder is averaged over due to thermal fluctuations within the pinning energy landscape. To make further progress we make two assumptions. First, we assume that $N(T)$ is reasonably large, which will be true for practically all $T>T^*$ due to the exponential increase in Eq. (65). Second, we assume that the $N(T)$ states the thermal fluctuations average over are drawn *randomly* from the distribution $p(E)$. This assumption is true at high temperatures when $T>|E_0|$; at low temperatures $T<|E_0|$ the thermal average will be only over the accessible states in the interval $[E_0,E_0+T]$ above the ground state. Under these assumptions, we can use the central limit theorem and introduce an effective thermally weakened pinning strength $\overline{U_p}$ which replaces the result (55) that is based on weak pinning assumptions:

$$\overline{U_p^2}(T)=U_p^2\frac{1}{N(T)}\simeq\begin{cases}T<|E_0|: & \left(1+\dfrac{T}{T^*}\right)^{-1}\exp\left(-\dfrac{T}{T^*}\right)\\ T>|E_0|: & \dfrac{T_{dp,d}}{T}.\end{cases} \tag{67}$$

Note that at $T \simeq |E_0|$, the high-temperature result crosses over to our above result (55) where we assumed the thermal smoothing to be independent of the disorder, which is only true for weak pinning. We noted already that for $T > T^*$ the displacement fluctuations are given by RF results. Whereas for weakly pinned pancake vortices ($\delta_d < 1$) the effective pinning strength (55) was appropriate which led to formula (57) or (58), we have to use the effective pinning strength (67) for strong pinning ($\delta_d > 1$) in the random force theory. This gives

$$\overline{\langle u \rangle^2}_{RF} \simeq \overline{\langle u \rangle^2}_{RF,T=0} \frac{1}{N^2(T)} \simeq \xi_{ab}^2 \delta_d \begin{cases} T < |E_0|: & \left(1 + \frac{T}{T^*}\right)^{-2} \exp\left(-2\frac{T}{T^*}\right) \\ T > |E_0|: & \left(\frac{T_{dp,d}}{T}\right)^2, \end{cases} \tag{68}$$

for the correct temperature dependence of the disorder-induced displacement fluctuations for pancakes for $T > T^*$ [again, as derivatives of the potential force correlations have an additional factor $N^{-1}(T)$ as compared to Eq. (67)]. Note that $\overline{\langle u \rangle^2}_{RF} < \langle u^2 \rangle_T$ for $T > T^*$ such that $\overline{\langle u^2 \rangle} \simeq \langle u \rangle_T^2$ for $T > T^*$ and disorder-induced fluctuations only dominate below T^*. At $T \simeq |E_0|$, the high-temperature result (68) crosses over to our above results (57) or (58).

We also realize that in Eq. (42), factors $(1 + \langle u^2 \rangle_T(d)/\xi_{ab}^2)$ which give the number of thermally accessible states in weak pinning theory should be replaced by $N(T)$ if we have strong pinning $\delta_d > 1$ [or $L_c(0) < d$]. Also thermal fluctuations of longer vortex segments $L > d$ have different behavior in the case of strong pinning. Thermal fluctuations of relative displacements in the different layers are independent which leads to $\langle u^2 \rangle_T(L) \simeq (L/d) \langle u^2 \rangle_T(d)$. Therefore, also the number of thermally accessible states adds up to

$$N(T,L) \simeq \frac{L}{d} N(T) \tag{69}$$

if $L > d$. Analogously to what we noted for the thermal smoothing on the scale d, factors $[1 + \langle u^2 \rangle_T(L)/\xi_{ab}^2]$ in the weak pinning result (42) have to be replaced by $N(T,L)$ in case of strong pinning.

Using Eq. (42) modified by this replacement and the definition of the pinning length by the relation $\overline{\langle u \rangle^2}(L_c(T)) \simeq \xi_{ab}^2 + \langle u^2 \rangle_T(L_c(T))$ we can obtain the thermal smoothing of the pinning length $L_c(T)$ for the case of strong pinning where $L_c(0) < d$ at low temperatures. First, we have observed above that the transition temperature T^* is exactly the temperature where $\overline{\langle u \rangle^2}_{RSB}(d) \simeq \langle u \rangle_T^2(d)$ such that

$$L_c(T^*) \simeq d \tag{70}$$

by definition of $L_c(T)$. It is also clear from Eqs. (65) and (69) that for $T > |E_0|$ the results for the thermal smoothing cross over to the weak pinning results. Therefore we recover cases (i) of the results (51) for weak Josephson coupling and (46) for strong Josephson coupling for $T > |E_0|$. The crossover within the temperature range $T^* < T < |E_0|$ is approximately described with the aid of our results (65) and (69) for $N(T,L)$, and gives a very steep increase from $L_c(T^*) \simeq d$ to the weak pinning results due to the exponential growth (65) of $N(T)$ in this temperature interval. For strong Josephson coupling $\varepsilon \lambda_{ab} > d$ we find

$$\text{(i):} \quad L_c(T) \simeq \begin{cases} T^*: & d \\ T^* < T < |E_0|: & d \max\left\{1, \frac{1}{N(T)} e^{(L_{c,\varepsilon}/d)^3 (T/T_{dp,d}) N(T)^2}\right\} \\ |E_0| < T < T_{\varepsilon\lambda}: & L_{c,\varepsilon} \frac{T_{dp,\varepsilon}}{T} e^{(T/T_{dp,\varepsilon})^3}, \end{cases} \tag{71}$$

whereas for a weak Josephson coupling $d > \varepsilon \lambda_{ab}$ we obtain

$$\text{(i):} \quad L_c(T) \simeq \begin{cases} T^{*-}: & d \\ T^{*+}: & L_{c,i} \delta_d^{1/6} \simeq \tilde{L}_c \delta_d^{-1/6} (< \tilde{L}_c) \\ T^* < T < |E_0|: & L_{c,i} N^{2/3}(T) \left(\frac{T}{T_{dp,d}}\right)^{1/3} \simeq \tilde{L} \frac{T^{1/3} T_{dp,d}^{2/3}}{T_{dp,i}} N^{2/3}(T) \\ |E_0| < T < T_{dp,i}: & \tilde{L}_c \frac{T}{T_d} \simeq \tilde{L} \frac{T}{T_{dp,i}}. \end{cases} \tag{72}$$

Note that $T^* > T_{dp,\varepsilon}$ for a strong Josephson coupling ($\varepsilon\lambda_{ab} > d$) such that the effective depinning temperature appears to be T^* as in the case of weak Josephson coupling. $L_c(T)$ grows with a double exponential for $T^* < T < |E_0|$ before we recover the weak pinning results (46) for $T > |E_0|$. Analyzing the modified relation (42) carefully, it becomes clear that approaching T^* from the high-temperature side we find $L_c(T) \simeq d$ already at a temperature $T \simeq T^* \ln\delta_d \ll |E_0|$. On the other hand we found in Eq. (70) that $L_c(T^*) \simeq d$. This suggests that $L_c(T) \simeq d$ not only for $T \ll T^*$ but that this relation extends into the temperature interval $T^* < T < |E_0|$ which is implied by the notation in the second line of Eq. (71). For a weak Josephson coupling ($d > \varepsilon\lambda_{ab}$) the electromagnetic coupling leads to a pronounced jump of the pinning length $L_c(T)$ at the temperature T^* from $L_c \simeq d$ to $L_c \simeq L_{c,i}\delta_d^{1/6}$, which is followed by an exponential increase up to $T \simeq |E_0|$ where we recover the weak pinning results (51). This jump is the analogon to what we found in Eq. (46) for a strong Josephson coupling. The result (72) for the pinning length for a weak Josephson coupling is in qualitative agreement but slightly different from what has been obtained previously in Ref. 9.

C. Thermal depinning in the random manifold regime

On scales $L < L_c(T)$ the disorder-induced displacements $\overline{\langle u\rangle^2}(L)$ are decreased by thermal smearing of the disorder potential according to Eq. (42) for $d < L < L_c(T)$ and weak collective pinning and according to Eq. (62) on the scale $L = d$ when we consider strongly pinned single-pancake vortices. Above the depinning temperature where L_c starts to increase from its $T = 0$ value, there is a range of length scales $L < L_c(T)$ where the disorder-induced displacements are smaller than the thermal displacements $\langle u^2\rangle_T(L)$ for weak collective pinning. However, on scales $L > L_c(T)$ for weak collective pinning and $L > d$ for strong pinning the disorder is still dominating and thermal fluctuations do not change the large-scale scaling properties in the RM regime as worked out in formulas (32), (33), and (38). However, we eventually have to adjust the normalization of the scaling relations. In the case of weak pinning $L_c(T) > d$ we normalize using $\overline{\langle u\rangle^2}(L_c(T)) \simeq \langle u^2\rangle_T(L_c(T))$ and obtain

$$\overline{\langle u\rangle^2}(L) \simeq \langle u^2\rangle_T(L_c(T)) \left(\frac{L}{L_c(T)}\right)^{2\zeta_{RM}} \tag{73}$$

in the nondispersive regimes $L_c(T) < L < \varepsilon\lambda_{ab}$ and $L > L_c(T) > \tilde{L}_c$. For strong pinning $L_c < d$ on scales $d < L < \varepsilon\lambda_{ab}$ the result (33) stays valid for temperatures $T < T^*$ where thermal smearing can be neglected. For $T > T^*$ the Larkin length increases beyond d due to thermal smearing and we can use the above weak pinning result (73) with $L_c(T)$ as crossover scale.

For the remaining dispersion-dominated case $L > L_c(T)$ when $\tilde{L}_c > L_d > L_c(T)$ the result (38) remains valid as all relevant length scales exceed $L_c(T)$ and thermal smearing can be neglected.

VI. CRITICAL CURRENTS

Each vortex configuration has a different pinning energy which gives rise to the quenched positional fluctuations of the vortex line that tries to optimize its pinning energy gain. The energy landscape in the high-dimensional configurational space is very complex (Fig. 2 illustrates the much simpler energy landscape of a pointlike pancake segment) leading to the existence of many metastable vortex configurations. If a current is applied there is an additional Lorentz force $f_L = j\Phi_0/c$ (per vortex length) on a pinned vortex segment and thus an energy gain $f_L L u$ for displacing a vortex segment of length L by an amount u. Therefore the pinning energy landscape becomes tilted in the presence of the driving force and eventually the optimal vortex configuration changes. In the absence of thermal fluctuations at $T = 0$, however, vortex motion does not set in as soon as the global energy minimum changes but only when the initial energy minimum becomes *unstable* due to the driving force exerted by the current. This happens if the Lorentz force f_L on the pinned vortex segment becomes larger than the average pinning force, which defines the *critical current density* j_c. For $j < j_c$ there are energy barriers between the metastable vortex configurations which diverge for small currents. These energy barriers can be overcome only by thermal activation for $T > 0$ giving rise to *vortex creep* for $j < j_c$. In the limit of small currents barriers diverge, and the activated creep dynamics becomes very slow which is a hallmark of glassy behavior. For $j > j_c$ the tilt of the energy landscape is sufficient that all barriers vanish and the vortex line starts to move with the usual *flux flow* velocity $v \sim j\rho_n/H_{c2}$, where ρ_n is the normal-state resistivity.

A. Weak collective pinning

In order to determine the critical current density we have to consider vortex displacements $u^2 \simeq \xi_{ab}^2 + \langle u^2\rangle_T(L_c)$, which are of the order of the disorder potential correlation length ξ_{ab} at low temperatures which gets smeared out by the thermal motion of the pinned vortex above the depinning temperature. For weak pinning $L_c(T) > d$ the optimal length of the displaced vortex segment is given by the pinning length $L_c(T)$. The typical *pinning energy variations* U_c encountered by displacing such a segment can be estimated from the elastic energy and Eq. (41) for strong Josephson coupling ($\varepsilon\lambda_{ab} > d$) as

$$\begin{aligned} U_c &\simeq q^2 \varepsilon_l(q) G_{RF}(q)\big|_{q=1/L_c(T)} \\ &\simeq \gamma \int_0^{L_c(T)} dl \, \frac{l}{\varepsilon_l(1/l)} \, \frac{\xi_{ab}^4}{[\xi_{ab}^2 + \langle u^2\rangle_T(l)]^2}, \end{aligned} \tag{74}$$

which gives

$$\text{(i):}\quad U_c \simeq \begin{cases} T < T_{dp,\varepsilon}: & T_{dp,\varepsilon} \\ T_{dp,\varepsilon} < T < T_{\varepsilon\lambda}: & T \\ T_{\varepsilon\lambda} < T < T_{dp,i}: & T_{dp,i} \\ T > T_{dp,i}: & T, \end{cases} \tag{75a}$$

$$\text{(ii),(iii):}\quad U_c \simeq \begin{cases} T<T_{dp,i}: & T_{dp,i} \\ T>T_{dp,i}: & T. \end{cases} \tag{75b}$$

First we note that at $T=0$, there is a jump in the characteristic energy from $U_c \simeq T_{dp,\varepsilon}$ to $U_c \simeq T_{dp,i}$ if we move from pinning regime (i) to regime (ii) by increasing the disorder strength. This happens because the Larkin length, which gives the length scale of the displaced vortex segment, jumps from $L_c(0)=\varepsilon\lambda_{ab}$ to $L_c(0)=\tilde{L}_c$ at this pinning strength $\delta=\delta_{\varepsilon\lambda}$. The behavior of the pinning energies as a function of temperature is determined by the two characteristic depinning temperatures $T_{dp,\varepsilon}$ and $T_{dp,i}$ for short-scale anisotropic stiffness and large-scale isotropic stiffness, respectively. Short-scale segments $L_c(T)<\varepsilon\lambda_{ab}$ thermally depin for $T>T_{dp,\varepsilon}$ and typical barriers are given by the temperature then. Most notable is the jump at the temperature $T_{\varepsilon\lambda}$ from a $U_c \simeq T_{\varepsilon\lambda}$ to the higher value $U_c \simeq T_{dp,i}$ which is due to the corresponding jump in the pinning length (46) and the accompanying increase in the stiffness $\varepsilon_l[1/L_c(T)]$. The larger segments $L_c(T)>\lambda_{ab}$ thermally depin only above the isotropic depinning temperature $T_{dp,i}$ which therefore sets again a typical pinning energy for $T_{\varepsilon\lambda}<T<T_{dp,i}$.

For a weak Josephson coupling ($d>\varepsilon\lambda_{ab}$) we obtain essentially the same result

$$\text{(i), (ii), (iii):}\quad U_c \simeq \begin{cases} T<T_{dp,i}: & T_{dp,i} \\ T>T_{dp,i}: & T \end{cases} \tag{76}$$

in all three cases (i)–(iii) but in case (i) of large disorder we have to consider sufficiently high temperatures $T>|E_0|$ such that $L_c(T)\gg d$, otherwise we are in the regime of strong pinning. As for a weak Josephson coupling there is also a jump in U_c at $T=0$ when we move from regime (i) to (ii) by increasing the disorder strength. This will become clear below from the $T=0$ results for strong pinning of single pancakes.

The corresponding energy gain from driving the segment of length $L_c(T)$ the distance $u(L_c(T))$ with $u^2(L_c(T)) \simeq \xi_{ab}^2 + \langle u^2\rangle_T(L_c(T))$ is $f_L L_c(T) u(L_c(T)) \simeq j L_c(T) u(L_c(T)) \Phi_0/c$. This energy gain balances the pinning energy variations U_c at the depinning threshold which gives a critical current

$$j_c \simeq \frac{c}{\Phi_0} U_c \frac{1}{L_c(T) u(L_c(T))}. \tag{77}$$

The jumps in $L_c(T)$ lead to characteristic drops in the critical current density as a function of temperature as reported for the case of vanishing Josephson coupling and strong pinning in Ref. 9. Putting the different results (75) for U_c, (46) for $L_c(T)$, and the corresponding expression for $u(L_c(T))$ together we find for strong Josephson coupling $\varepsilon\lambda_{ab}>d$,

$$\text{(i):}\quad j_c \simeq \begin{cases} T<T_{dp,\varepsilon}: & j_{c,\varepsilon} \simeq j_0 \left(\dfrac{\delta}{\varepsilon}\right)^{2/3} \\ T_{dp,\varepsilon}<T<T_{\varepsilon\lambda}: & j_{c,\varepsilon}\left(\dfrac{T}{T_{dp,\varepsilon}}\right)^2 e^{-\frac{3}{2}(T/T_{dp,\varepsilon})^3} \\ T=T_{\varepsilon\lambda}^-: & j_0\left(\dfrac{T_{\varepsilon\lambda}}{\varepsilon_0\xi_{ab}}\right)^{1/2}\left(\dfrac{\xi_{ab}}{\varepsilon\lambda_{ab}}\right)^{3/2}\varepsilon \\ T=T_{\varepsilon\lambda}^+: & j_0\left(\dfrac{T_{\varepsilon\lambda}}{\varepsilon_0\xi_{ab}}\right)^{1/2}\dfrac{T_{dp,i}}{T_{\varepsilon\lambda}}\left(\dfrac{\xi_{ab}}{\varepsilon\lambda_{ab}}\right)^{3/2}\varepsilon^{7/3} \\ T_{\varepsilon\lambda}^+<T<T_{dp,i}: & j_0\left(\dfrac{T}{\varepsilon_0\xi_{ab}}\right)^{1/2}\left(\dfrac{T_{dp,i}}{T}\right)^2\left(\dfrac{\xi_{ab}}{\tilde{L}}\right)^{3/2} \\ T>T_{dp,i}: & j_0\left(\dfrac{T}{\varepsilon_0\xi_{ab}}\right)^{1/2}\left(\dfrac{\xi_{ab}}{\tilde{L}}\right)^{3/2} e^{-(3/2)(T/T_{dp,i})^3} \\ & \simeq j_{c,i}\left(\dfrac{T}{T_{dp,i}}\right)^{1/2}\left(\dfrac{T_{dp,i}}{T_{dp,\varepsilon\lambda}}\right)^{-3/2} e^{-(3/2)(T/T_{dp,i})^3}, \end{cases} \tag{78a}$$

$$\text{(ii):}\quad j_c \simeq \begin{cases} T<T_{dp,\varepsilon\lambda}: & j_{c,i} \simeq j_0\left(\dfrac{T_{dp,i}}{\varepsilon_0\xi_{ab}}\right)^{1/2}\left(\dfrac{\xi_{ab}}{L_{c,i}}\right)^{3/2} \simeq j_0\delta^{2/3} = \varepsilon^{2/3} j_{c,\varepsilon} \\ T_{dp,\varepsilon\lambda}<T<T_{dp,i}: & j_{c,i}\left(\dfrac{T_{dp,\varepsilon\lambda}}{T}\right)^{3/2} \\ T>T_{dp,i}: & j_{c,i}\left(\dfrac{T}{T_{dp,i}}\right)^{1/2}\left(\dfrac{T_{dp,i}}{T_{dp,\varepsilon\lambda}}\right)^{-3/2} e^{-(3/2)(T/T_{dp,i})^3}, \end{cases} \tag{78b}$$

$$\text{(iii)}: \quad j_c \simeq \begin{cases} T<T_{dp,i}: & j_{c,i} \\ T_{dp,i}<T<T_{dp,\varepsilon\lambda}: & j_{c,i}\left(\dfrac{T}{T_{dp,i}}\right)^2 e^{-(3/2)(T/T_{dp,i})^3} \\ T>T_{dp,\varepsilon\lambda}: & j_{c,i}\left(\dfrac{T}{T_{dp,i}}\right)^{1/2}\left(\dfrac{T_{dp,i}}{T_{dp,\varepsilon\lambda}}\right)^{-3/2} e^{-(3/2)(T/T_{dp,i})^3}, \end{cases} \tag{78c}$$

where $j_0 \simeq c\varepsilon_0/\Phi_0\xi_{ab}$ is the depairing current. The different regimes in the temperature dependence of the critical current density j_c for strong Josephson coupling are illustrated in Fig. 4(a). Most notably, there is a pronounced drop of the critical current by a factor of $\varepsilon^{4/3}$ at $T_{\varepsilon\lambda}$ in case (i) of large disorder which should be observable at low-field experiments.

Using Eqs. (76) and (51) results for weak Josephson coupling $d>\varepsilon\lambda_{ab}$ are completely analogous to formulas (78). The basic differences are the different definition of the thermal plateau length $\tilde{L}$, see Eq. (11), and that in regimes (ii) and (iii) thermal depinning is now governed by the length scale d and the corresponding temperature $T_{dp,d}$. Within weak pinning theory we are limited to temperatures $T>|E_0|$ where we find

$$\text{(i)}: \quad j_c \simeq \begin{cases} T<T_{dp,i}: & j_0\left(\dfrac{T}{\varepsilon_0\xi_{ab}}\right)^{1/2}\left(\dfrac{T_{dp,i}}{T}\right)^2\left(\dfrac{\xi_{ab}}{\tilde{L}}\right)^{3/2} \\ T>T_{dp,i}: & j_0\left(\dfrac{T}{\varepsilon_0\xi_{ab}}\right)^{1/2}\left(\dfrac{\xi_{ab}}{\tilde{L}}\right)^{3/2} e^{-(3/2)(T/T_{dp,i})^3} \\ & \simeq j_{c,i}\left(\dfrac{T}{T_{dp,i}}\right)^{1/2}\left(\dfrac{T_{dp,i}}{T_{dp,d}}\right)^{-3/2} e^{-(3/2)(T/T_{dp,i})^3}, \end{cases} \tag{79a}$$

$$\text{(ii)}: \quad j_c \simeq \begin{cases} T<T_{dp,d}: & j_{c,i} \\ T_{dp,d}<T<T_{dp,i}: & j_{c,i}\left(\dfrac{T_{dp,d}}{T}\right)^{3/2} \\ T>T_{dp,i}: & j_{c,i}\left(\dfrac{T}{T_{dp,i}}\right)^{1/2}\left(\dfrac{T_{dp,i}}{T_{dp,d}}\right)^{-3/2} e^{-(3/2)(T/T_{dp,i})^3}, \end{cases} \tag{79b}$$

$$\text{(iii)}: \quad j_c \simeq \begin{cases} T<T_{dp,i}: & j_{c,i} \\ T_{dp,i}<T<T_{dp,d}: & j_{c,i}\left(\dfrac{T}{T_{dp,i}}\right)^2 e^{-(3/2)(T/T_{dp,i})^3} \\ T>T_{dp,d}: & j_{c,i}\left(\dfrac{T}{T_{dp,i}}\right)^{1/2}\left(\dfrac{T_{dp,i}}{T_{dp,d}}\right)^{-3/2} e^{-(3/2)(T/T_{dp,i})^3}. \end{cases} \tag{79c}$$

Figure 4(b) shows the different regimes in the temperature dependence of the critical current density j_c for weak Josephson coupling. Case (i) of strong pinning is discussed in detail in the following section.

B. Strong pinning

For strong pinning $L_c<d$ we first focus on the behavior at low temperatures $T<T^*$. As the pinning length L_c exceeds the layer spacing, the optimal length of the displaced vortex segment is the minimal accessible length $L=d$ of a single-pancake segment. We have shown in Secs. IV B and V B that the energy landscape for a strongly pinned pancake segment is characterized by two energies. The pancake segment can attain a ground-state energy E_0 in the deepest traps of the energy landscape [see Eq. (29)]. The ground state is separated from metastable states by energy barriers of the order of $T^*=U^*$ [see Eqs. (30) and (61)]. A vortex in the ground state within an energy valley of size ξ_{ab} therefore experiences a typical pinning force $|E_0|/\xi_{ab}$. Driving forces $f_L d = jd\Phi_0/c > |E_0|/\xi_{ab}$ exceeding this value are needed to tilt the energy landscape such that all barriers vanish. Then the critical current for strong pinning is[9]

$$j_c \simeq \frac{c}{\Phi_0}|E_0|\frac{1}{d\xi_{ab}} \simeq j_d \ln^{1/2}\delta_d, \tag{80}$$

at low temperatures, where

$$j_d = j_0\frac{U_p}{\varepsilon_0 d} \tag{81}$$

is a characteristic current strength that is a convenient measure for critical currents at strong pinning [$j_d \approx j_0\kappa\delta_d^{1/2}$ for weak Josephson coupling $d>\varepsilon\lambda_{ab}$].

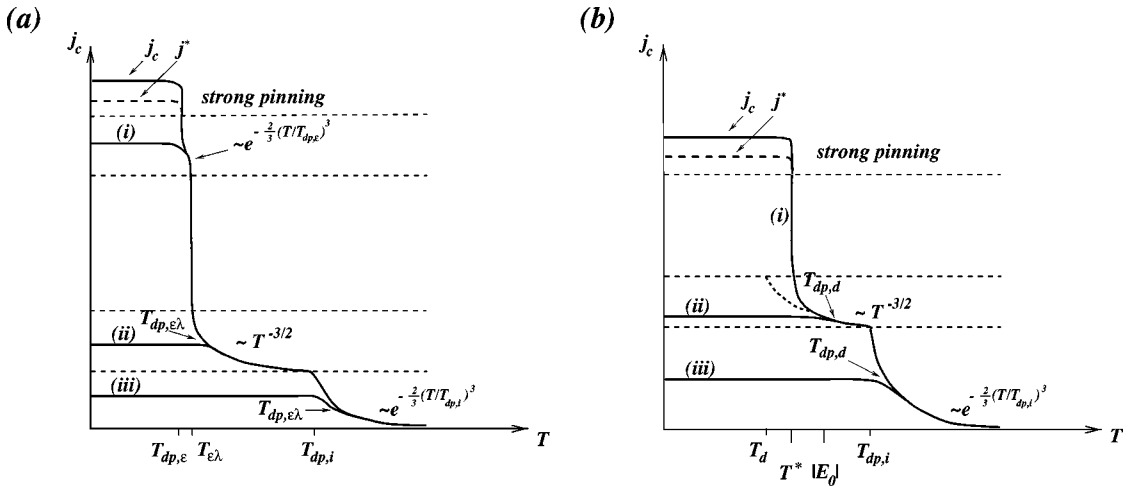

FIG. 4. Schematic plot of the temperature dependence of the critical current j_c (a) for strong Josephson coupling $\varepsilon\lambda_{ab}>d$ (e.g., for YBCO) according to Eq. (78) and (b) for weak Josephson coupling $d>\varepsilon\lambda_{ab}$ (e.g., for BSCCO) according to Eq. (79). j_c is limited by the low-temperature strong pinning result (80) which gives the solid line at the top; the barrier current strength j^* according to Eq. (82) gives the dashed line slightly below. Slightly above the temperature T^* the difference between j^* and j_c vanishes. The corresponding temperature-dependent curves for the case of strong pinning according to Eq. (86) emerge from this line at $T=T^*$.

If the current is decreased below the value of j_c given by Eq. (80) at low temperatures $T<T^*$, pancake segments have to overcome energy barriers by thermal activation. However, it is a hallmark of the strong pinning system that there exists a range of currents $j^*<j<j_c$ for which these barriers are independent of the current density j as the optimal length of the displaced segment stays at the minimal accessible length $L=d$. Only below the characteristic *pancake barrier current strength* j^*, the optimal length of the displaced vortex segment grows beyond the layer spacing d. This crossover current strength j^* is obtained by balancing the typical pinning energy variations U^* on the scale d against the energy gain from driving the pancake vortex over a typical displacement distance $u(d)=\overline{\langle u^2\rangle}(d)$, as calculated in Eq. (28). This gives[9]

$$j^*\simeq\frac{c}{\Phi_0}U^*\frac{1}{du(d)}\simeq j_d\delta_d^{-1/4}\ln^{-1/4}\delta_d, \tag{82}$$

which is well below j_c. As barriers to vortex motion are existing in the regime $j^*<j<j_c$ we do not identify j^* with the actual critical current as it has been done in Ref. 9.

At temperatures $T>T^*$ above the characteristic temperature T^* for the depinning of pancake segments *both* j_c and j^* decrease due to thermal smearing. For $T>T^*$ we find $L_c(T)>L_c(T^*)\simeq d$ [see Eq. (70)] and expect a crossover to our above results (78) for strong Josephson coupling and (79) for weak Josephson coupling. It can be shown that the critical current j_c is also for $T>T^*$ still determined by the Lorentz force necessary to drive small pancake segments of length $L=d$, however, due to thermal smearing the pinning energy $|E_0|$ of a single-pancake segment is reduced by a factor $N(T)$ as calculated in Eq. (65). Furthermore, we have to use a driving distance $u(d)$ with $u^2(d)\simeq\xi_{ab}^2+\langle u^2\rangle_T(d)$, and obtain

$$j_c\simeq\frac{c}{\Phi_0}\frac{|E_0|}{N(T)}\frac{1}{du(d)}, \tag{83}$$

which gives a j_c that is exponentially decreasing upon increasing the temperature above T^*. Due to this sharp drop the strong pinning result (83) crosses over to the weak pinning results (78) and (79) [that are only weakly temperature dependent] already slightly above T^*. The current j^*, on the other hand, crosses smoothly over to the weak pinning results (78) and (79) for j_c right at the temperature T^* where $U^*\simeq T^*$ and $L_c(T^*)\simeq d$. We will see that the result for j^* decreases much slower than j_c for temperatures slightly above T^*. Therefore, the range of currents $j^*<j<j_c$ where the energy barriers are j independent vanishes when j^* and j_c coincide which happens at a temperature only slightly above T^*. At higher temperatures we have $j_c=j^*$.

j^* is determined from the energy balance for optimal segments of size $L_c(T)$ that are driven a distance $u(L_c(T))$ with $u^2(L_c(T))\simeq\xi_{ab}^2+\langle u^2\rangle_T(L_c(T))$. Using the result (42) for $L_C(T)<d$, modified by the replacement of thermal smoothing factors by $N(T,L)$, we find for the corresponding characteristic energy scale

$$\text{(i): } U_c\simeq\begin{cases}T<T^*: & U^*\simeq T^*\\ T^*<T: & T\end{cases} \tag{84}$$

for $\varepsilon\lambda_{ab}>d$ and

$$\text{(i): } U_c\simeq\begin{cases}T<T^*: & U^*\simeq T^*\\ T^*<T: & T_{dp,i}\end{cases} \tag{85}$$

for $d>\varepsilon\lambda_{ab}$. We note that a jump of U_c happens for weak Josephson coupling in the strong-coupling regime at the temperature T^* where U_c increases from $U_c\simeq T^*$ to U_c

$\simeq T_{dp,i}$. To calculate j^* for $T>T^*$ we then use Eq. (77) but in connection with the results (84) and (85) for U_c and (71) and (72) for $L_c(T)$ appropriate for strong pinning. For strong Josephson coupling $\varepsilon\lambda_{ab}>d$ we obtain

$$\text{(i):}\quad j^*\simeq\begin{cases} T^*: & j_d\delta_d^{-1/4}\ln^{-1/4}(\delta_d^{1/2}) \\ T^*<T<|E_0|: & j_d\dfrac{T}{U_p}\left(\dfrac{T_{dp,d}}{T}\right)^{1/2}\min\{1,N^{3/2}(T)e^{-(3/2)(L_{c,\varepsilon}/d)^3(T/T_{dp,d})N(T)^2}\} \\ |E_0|<T<T_{\varepsilon\lambda}: & j_{c,\varepsilon}\left(\dfrac{T}{T_{dp,\varepsilon}}\right)^2 e^{-(3/2)(T/T_{dp,\varepsilon})^3} \end{cases} \tag{86a}$$

and for a weak Josephson coupling $d>\varepsilon\lambda_{ab}$ we find

$$\text{(i):}\quad j^*\simeq\begin{cases} T^{*-}: & j_d\delta_d^{-1/4}\ln^{-1/4}(\delta_d^{1/2}) \\ T^{*+}: & j_{c,i}\left(\dfrac{T^*}{T_{dp,d}}\right)^{-5/6}\simeq j_{c,i}\delta_d^{-5/12}\ln^{5/12}(\delta_d^{1/2}) \\ T^*<T<|E_0|: & j_{c,i}N^{-2/3}(T)\left(\dfrac{T}{T_{dp,d}}\right)^{-5/6} \\ |E_0|<T<T_{dp,i}: & j_0\left(\dfrac{T}{\varepsilon_0\xi_{ab}}\right)^{1/2}\left(\dfrac{T_{dp,i}}{T}\right)^2\left(\dfrac{\xi_{ab}}{\tilde{L}}\right)^{3/2}. \end{cases} \tag{86b}$$

Again, there is a pronounced drop of the critical current for a weak Josephson coupling ($d>\varepsilon\lambda_{ab}$) at the temperature T^* by a factor of $j_{c,i}\delta_d^{-1/6}/j_d\simeq\varepsilon_d\kappa^{-1}\delta_d^{-1/3}$. This is the analogon to our above findings in formulas (78) for a strong Josephson coupling.

VII. CURRENT-VOLTAGE CHARACTERISTICS

From the experimental point of view our results have interesting consequences for the interpretation of current-voltage characteristics in the low-field regime $B<\Phi_0/\lambda_{ab}^2$. For weak collective pinning the critical current j_c marks the crossover from a regime of glassy creep behavior at low currents $j<j_c$ to a flux flow regime at high currents $j>j_c$. For a given current density $j<j_c$ there is an optimal segment length $L(j)$ and a characteristic displacement $u(L(j))$ separating metastable configurations for which the energy gain $f_L L(j)u(L(j))$ is sufficient to overcome the pinning energy barriers $U(L(j))$ between the metastable states. Usually the barrier height $U(L(j))$ diverges as the length scale $L(j)$ diverges for small j giving rise to typical glassy creep behavior. Thus we have nonzero ohmic resistivity in the flux flow regime $j>j_c$ and a vanishing ohmic resistivity for small $j<j_c$ due to diverging energy barriers. Both strong pinning and electromagnetic coupling along a single-vortex line lead to two distinct features in the current-voltage characteristics at low fields.

We have already seen that for strong pinning of pancake vortices a novel current regime $j^*<j<j_c$ emerges where pancake vortices have to activate over barriers as in the typical creep scenario but where the barrier height is independent from j. This leads to the appearance of a second regime with *linear* current-voltage characteristics[9] as in the flux flow regime but which is nevertheless dominated by activation over barriers. This regime should be observable in experiments for temperatures $T<T^*$.

Furthermore, we can predict jumplike features in the current-voltage characteristics if pinning is such that $L_c<L_d$ [strong pinning or case (i) of large disorder for weak pinning, see definition (43)] at low temperatures. Similar to the jumps in the Larkin-length $L_c(T)$ as a function of temperature that we have found in Eqs. (46), (71), and (72) for this situation also the optimal segment length for the vortex line activation will jump from a value $L(j)=L_d$ to a larger value $L(j)>\lambda_{ab}$ at a particular current strength below j_c. As also the height of the corresponding pinning energy barrier $U(L(j))$ has a characteristic jump at this current strength, a jump should also be observable in the current-voltage characteristics as a qualitative feature. This finding holds for temperatures such that $L_c(T)<L_d$, i.e., for $T<T_{\varepsilon\lambda}$ for a strong Josephson coupling and for $T<T^*$ for a weak Josephson coupling.

VIII. CONCLUSION

We have provided a complete analysis of the displacement fluctuations of a pinned single-vortex line in a layered type-II superconductor including a detailed treatment of the electromagnetic coupling and the strong pinning regime. Due to the existence of four characteristic length scales—the layer spacing d, the length scale $\varepsilon\lambda_{ab}$ below which the Josephson coupling dominates, the magnetic penetration depth below which electromagnetic dispersion sets in, and the pinning length L_c characterizing the disorder strength—the behavior is very rich. The electromagnetic interaction leads to an effective decoupling of the layers for thermal fluctuations

with wavelengths L in the plateau regime $\varepsilon\lambda_{ab}<L<\tilde{L}$ and for disorder-induced fluctuations in the plateau regime $\varepsilon\lambda_{ab}<L<\tilde{L}_c$. The extent of these plateau regimes is characterized by two plateau crossover scales $\tilde{L}$ and $\tilde{L}_c$, see Eqs. (11) and (21), respectively. In our analysis we considered layered type-II superconductors both with strong Josephson coupling ($\varepsilon\lambda_{ab}>d$), such as YBCO, and with weak Josephson coupling ($d>\varepsilon\lambda_{ab}$), such as BSCCO. Regarding the influence of the line tension dispersion due to the electromagnetic coupling both kinds of materials behave rather similarly with length scales $\varepsilon\lambda_{ab}$ and d playing analogous roles. This can be seen in the definition (4) of the length scale L_d and in the definitions (11) and (21) of the thermal plateau length $\tilde{L}$ and the pinning plateau length $\tilde{L}_c$. Effects of the nonlocal electromagnetic coupling occur if the single-vortex length L_0 [see Eq. (8)] exceeds the dispersion length scale L_d. This condition is fulfilled in the low-field regime $B<\Phi_0/\lambda_{ab}^2$.

The existence of plateaus in positional fluctuations gives rise to ''jumps'' in the pinning length L_c as a function of disorder strength and temperature as well as to accompanying ''drops'' in the critical current density. These jumplike features occur if the pinning length is smaller than the dispersion length scale at low temperatures, i.e., for $L_c(0)<L_d$. This is the case in the strong pinning regime for BSCCO where $L_c<d$ or in the weak collective pinning regime in YBCO for case (i) of a large disorder according to the definition (43). The jumps will occur at temperatures where $L_c(T)=L_d$, i.e., where the pinning length becomes comparable to the dispersion length scale. For a strong Josephson coupling (as in YBCO) this is the temperature $T_{\varepsilon\lambda}$ at which $L_c(T_{\varepsilon\lambda})=\varepsilon\lambda_{ab}$ and for which we derived expression (48) using weak collective pinning theory. For a weak Josephson coupling (as in BSCCO) the analogous temperature is the temperature T^*, see Eq. (61); using strong pinning theory we have shown that $L_c(T^*)=d$. We find that the critical current can easily drop by one order of magnitude in a layered HTSC around these temperatures. Similar to the jumps in the Larkin length, we also predict jumps in the current-voltage characteristics which are due to jumps in the length of optimal segment for vortex line activation.

To allow comparison with experiments we give some estimates for the characteristic temperatures where we expect the critical current to drop [note that we take into account the temperature dependence of the microscopic parameters λ_{ab} and ξ_{ab} and calculate these temperatures self-consistently, the given values for λ_{ab} and ξ_{ab} are for $T=0$]. Taking typical values for YBCO as a layered HTSC with strong Josephson coupling, $\lambda_{ab}\approx 1500$ Å, $\varepsilon\approx 1/5$, $d\approx 12$ Å, and a disorder strength $\delta/\varepsilon\approx 5\times 10^{-3}$, we have weak pinning ($\delta_d<1$) and find $T_{dp,\varepsilon}\simeq 35$ K for the anisotropic depinning temperature, $T_{dp,i}\simeq 67$ K for the isotropic depinning temperature. The low-field regime, in which our results should be experimentally observable, is $B<\Phi_0/\lambda_{ab}^2\approx 900$ G for YBCO. The parameter values for YBCO are typically such that within the weak collective pinning regime it is indeed in regime (i) of large disorder, i.e., $L_c(0)<L_d$ according to the definition (43). Using the above parameter values for YBCO we find $L_c(0)=L_{c,\varepsilon}(0)\approx 18$ Å and $L_d=\varepsilon\lambda_{ab}\approx 300$ Å. Therefore, a drop of the critical current should be observable in low-field experiments on YBCO. For YBCO this drop is predicted to occur around a temperature $T_{\varepsilon\lambda}\approx 45$ K. We also expect that jumplike features in the current-voltage characteristics are observable for temperatures $T<T_{\varepsilon\lambda}$.

For typical values for BSCCO as a layered HTSC with weak Josephson coupling [below $T_{d,J}\approx 55$ K, see Eq. (6)], $\lambda_{ab}\approx 2000$ Å, $\varepsilon\approx 1/200$, $d\approx 15$ Å, and using the same δ as for YBCO, we find disorder strengths $\delta/\varepsilon\approx 2\times 10^{-1}$ and are in the strong pinning regime where $\delta_d\gg 1$. The low-field regime, where our results should be observable, is $B<\Phi_0/\lambda_{ab}^2\approx 500$ G in BSCCO. We obtain $U_p\approx 22$ K for the strong pinning energy scale, $T_{dp,i}\simeq 61$ K for the isotropic depinning temperature; the barrier height $T^*\approx 11$ K and the ground-state energy $|E_0|\approx 42$ K give a range of temperatures in which the critical current density will drop. As opposed to YBCO, such drops in the critical current around $T\simeq 20$ K have already been observed experimentally for BSCCO.[8] As for YBCO, we also predict that jumplike features in the current-voltage characteristics are observable for BSCCO. They should occur in the temperature range $T<T^*\approx 11$ K.

The other focus of the present analysis were the properties of the regime of strong pinning of pancake segments in layered type-II superconductors, which occurs for $L_c<d$, i.e., if the pinning length becomes smaller than the layer spacing. In principle, strong pinning can occur both for strong and weak Josephson coupling. However, the layered pinning strength parameter δ_d is typically much larger in BSCCO due to the smaller values of ϵ, cf. Eq. (16). Therefore, we typically have strong pinning only in BSCCO. Measurements of the magnetic susceptibility provide a probe of the depth of pinning energy minima.[7,8] Using this technique the crossover from weak pinning of vortex lines to strong pinning of point-like pancake vortices has been observed for BSCCO.[7,8] According to our results this transition happens also in the temperature range $T^*<T<|E_0|$. In Ref. 7 the transition to strong pinning of pancakes has been observed for temperatures $T\simeq 20$ K also supporting our results. For YBCO disorder strengths are usually too small to find strong pinning of single pancakes. However, it might be possible to increase the point disorder strength using proton irradiation[25] to a level where strong pinning effects could be observed also in YBCO.

Furthermore, results obtained in this paper will be of future use in calculating the low-field part of the vortex phase diagram of layered type-II superconductors by using Lindemann criteria.

ACKNOWLEDGMENTS

The author thanks A. E. Koshelev and V. M. Vinokur for numerous discussions on the subject, acknowledges the Argonne National Laboratory for hospitality, and the Deutsche Forschungsgemeinschaft for support through Grant No. KI 662/1 in the early stages of this work.

[1] G. Blatter, M.V. Feigelman, V.B. Geshkenbein, A.I. Larkin, and V.M. Vinokur, Rev. Mod. Phys. **66**, 1125 (1994).
[2] E.H. Brandt, Rep. Prog. Phys. **58**, 1465 (1995).
[3] T. Nattermann and S. Scheidl, Adv. Phys. **49**, 607 (2000).
[4] A.I. Larkin, Zh. Eksp. Teor. Fiz. **58**, 1466 (1970) [Sov. Phys. JETP **31**, 784 (1970)]; A.I. Larkin and Y.N. Ovchinnikov, J. Low Temp. Phys. **34**, 409 (1979).
[5] C.J. van der Beek, M. Konczykowski, A. Abal'oshev, I. Abal'osheva, P. Gierlowski, S.J. Lewandowski, M.V. Indenbom, and S. Barbanera, Phys. Rev. B **66**, 024523 (2002).
[6] M. Nideröst, A. Suter, P. Visani, A.C. Mota, and G. Blatter, Phys. Rev. B **53**, 9286 (1996).
[7] M.F. Goffman, J.A. Herbsommer, F. de la Cruz, T.W. Li, and P.H. Kes, Phys. Rev. B **57**, 3663 (1998).
[8] V.F. Correa, J.A. Herbsommer, E.E. Kaul, F. de la Cruz, and G. Nieva, Phys. Rev. B **63**, 092502 (2001).
[9] O.S. Wagner, G. Burkard, V.B. Geshkenbein, and G. Blatter, Phys. Rev. Lett. **81**, 906 (1998).
[10] A. Houghton, R.A. Pelcovits and A. Sudbø, Phys. Rev. B **40**, 6763 (1989); G. Blatter, V. Geshkenbein, A. Larkin, and H. Nordborg, *ibid.* **54**, 72 (1996).
[11] D. Ertaş and D.R. Nelson, Physica C **272**, 79 (1996); Y.Y. Goldschmidt, Phys. Rev. B **56**, 2800 (1997); T. Giamarchi and P. Le Doussal, *ibid.* **55**, 6577 (1997); A.E. Koshelev and V.M. Vinokur, *ibid.* **57**, 8026 (1998); V. Vinokur, B. Khaykovich, E. Zeldov, M. Konczykowski, R.A. Doyle, and P.H. Kes, Physica C **295**, 209 (1998); J. Kierfeld, *ibid.* **300**, 171 (1998); G.P. Mikitik and E.H. Brandt, Phys. Rev. B **64**, 184514 (2001).
[12] J.R. Clem, Phys. Rev. **43**, 7837 (1991).
[13] J. Kierfeld, Physica C **300**, 171 (1998).
[14] J. Kierfeld and V. Vinokur, Phys. Rev. B **69**, 024501 (2004).
[15] G. Blatter, V. Geshkenbein, A. Larkin, and H. Nordborg, Phys. Rev. B **54**, 72 (1996).
[16] D.A. Huse, C.L. Henley, and D.S. Fisher, Phys. Rev. Lett. **55**, 2924 (1985).
[17] J.M. Kim and J.M. Kosterlitz, Phys. Rev. Lett. **62**, 2289 (1989).
[18] T. Halpin-Healy and Y.C. Zhang, Phys. Rep. **254**, 215 (1995).
[19] A.E. Koshelev, L.I. Glazman, and A.I. Larkin, Phys. Rev. B **53**, 2786 (1996).
[20] A.E. Koshelev and V.M. Vinokur, Phys. Rev. B **57**, 8026 (1998).
[21] A. Engel, Nucl. Phys. B **410**, 617 (1993).
[22] D.S. Fisher, M.P.A. Fisher, and D.A. Huse, Phys. Rev. B **43**, 130 (1991).
[23] T. Hwa and D.S. Fisher, Phys. Rev. B **49**, 3136 (1994).
[24] T. Giamarchi and P. Le Doussal, Phys. Rev. B **52**, 1242 (1995).
[25] A.M. Petrean, L.M. Paulius, W.-K. Kwok, J.A. Fendrich, and G.W. Crabtree, Phys. Rev. Lett. **84**, 5852 (2000).